

ELECTROWEAK PRECISION TESTS: A CONCISE REVIEW¹

G. Altarelli

Theoretical Physics Division, CERN
CH - 1211 Geneva 23
and
Università di Roma Tre, Rome, Italy

R. Barbieri

Scuola Normale Superiore, Pisa, Italy
and
INFN, Sezione di Pisa, Italy

F. Caravaglios

Theoretical Physics Division, CERN
CH - 1211 Geneva 23

Content

1. Introduction
2. Status of the Data
3. Precision Electroweak Data and the Standard Model
4. A More General Analysis of Electroweak Data
 - 4.1 Basic Definitions and Results
 - 4.2 Experimental Determination of the Epsilon Variables
 - 4.3 Comparing the Data with the Minimal Supersymmetric Standard Model
5. Theoretical Limits on the Higgs Mass
6. Conclusion

Submitted to Int. Journal of Modern Physics A

CERN-TH/97-290
SNS/PH/1997-7
October 1997

¹This work is partially supported by the "Beyond the Standard Model" TMR network under the EEC contract No. ERBFMRX-CT960090.

1 Introduction

In recent years new powerful tests of the Standard Model (SM) have been performed mainly at LEP but also at SLC and at the Tevatron. The running of LEP1 was terminated in 1995 and close-to-final results of the data analysis are now available [1],[2]. The experiments at the Z_0 resonance have enormously improved the accuracy in the electroweak neutral current sector. The top quark has been at last found and the errors on m_Z and $\sin^2 \theta_{eff}$ went down by two and one orders of magnitude, respectively, since the start of LEP in 1989. The LEP2 programme is in progress. The validity of the SM has been confirmed to a level that we can say was unexpected at the beginning. In the present data there is no significant evidence for departures from the SM, no convincing hint of new physics (also including the first results from LEP2) [3]. The impressive success of the SM poses strong limitations on the possible forms of new physics. Favoured are models of the Higgs sector and of new physics that preserve the SM structure and only very delicately improve it, as is the case for fundamental Higgs(es) and Supersymmetry. Disfavoured are models with a nearby strong non perturbative regime that almost inevitably would affect the radiative corrections, as for composite Higgs(es) or technicolor and its variants[4]-[6].

2 Status of the Data

The relevant electro-weak data together with their SM values are presented in table 1 [1]-[2]. The SM predictions correspond to a fit of all the available data (including the directly measured values of m_t and m_W) in terms of m_t , m_H and $\alpha_s(m_Z)$, described later in sect.3, table 4 (last column).

Other important derived quantities are, for example, N_ν the number of light neutrinos, obtained from the invisible width: $N_\nu = 2.993(11)$, which shows that only three fermion generations exist with $m_\nu < 45$ GeV, or the leptonic width Γ_l , averaged over e, μ and τ : $\Gamma_l = 83.91(10)MeV$, or the hadronic width: $\Gamma_h = 1743.2(2.3)$ MeV.

For indicative purposes, in table 1 the "pulls" are also shown, defined as: pull = (data point- fit value)/(error on data point). At a glance we see that the agreement with the SM is quite good. The distribution of the pulls is statistically normal. The presence of a few $\sim 2\sigma$ deviations is what is to be expected. However it is maybe worthwhile to give a closer look at these small discrepancies.

Perhaps the most annoying feature of the data is the persistent difference between the values of $\sin^2 \theta_{eff}$ measured at LEP and at SLC. The value of $\sin^2 \theta_{eff}$ is obtained from a set of combined asymmetries. From asymmetries one derives the ratio $x = g_V^l/g_A^l$ of the vector and axial vector couplings of the Z_0 , averaged over the charged leptons. In turn $\sin^2 \theta_{eff}$ is defined by $x = 1 - 4 \sin^2 \theta_{eff}$. SLD obtains x from the single measurement of A_{LR} , the left-right asymmetry, which requires longitudinally polarized beams. The distribution of the present measurements of $\sin^2 \theta_{eff}$ is shown in fig. 1. The LEP average, $\sin^2 \theta_{eff} = 0.23199(28)$, differs

by 2.9σ from the SLD value $\sin^2 \theta_{eff} = 0.23055(41)$. The most precise individual measurement at LEP is from A_b^{FB} : the combined LEP error on this quantity is about the same as the SLD error, but the two values are 3.1σ 's away. One might attribute this to the fact that the b measurement is more delicate and affected by a complicated systematics. In fact one notices from fig. 1 that the value obtained at LEP from A_l^{FB} , the average for $l=e, \mu$ and τ , is somewhat low (indeed quite in agreement with the SLD value). However the statement that LEP and SLD agree on leptons while they only disagree when the b quark is considered is not quite right. First, the value of A_e , a quantity essentially identical to A_{LR} , measured at LEP from the angular distribution of the τ polarization, differs by 1.8σ from the SLD value. Second, the low value of $\sin^2 \theta_{eff}$ found at LEP from A_l^{FB} turns out to be entirely due to the τ lepton channel which leads to a central value different than that of e and μ [2]. The e and μ asymmetries, which are experimentally simpler, are perfectly on top of the SM fit. Suppose we take only e and μ asymmetries at LEP and disregard the b and τ measurements: the LEP average becomes $\sin^2 \theta_{eff} = 0.23184(55)$, which is still 1.9σ away from the SLD value.

In conclusion, it is difficult to find a simple explanation for the SLD-LEP discrepancy on $\sin^2 \theta_{eff}$. In view of this, the error on the nominal SLD-LEP average, $\sin^2 \theta_{eff} = 0.23152(23)$, should perhaps be enlarged, for example, by a factor $S = \sqrt{\chi^2/N_{df}} \sim 1.4$, according to the recipe adopted by the Particle Data Group in such cases. Accordingly, in the following we will often use the average

$$\sin^2 \theta_{eff} = 0.23152 \pm 0.00032 \quad (1)$$

Thus the LEP-SLC discrepancy results in an effective limitation of the experimental precision on $\sin^2 \theta_{eff}$. The data-taking by the SLD experiment is still in progress and also at LEP sizeable improvements on A_τ and A_b^{FB} are foreseen as soon as the corresponding analyses will be completed. We hope to see the difference to decrease or to be understood.

From the above discussion one may wonder if there is evidence for something special in the τ channel, or equivalently if lepton universality is really supported by the data. Indeed this is the case: the hint of a difference in A_τ^{FB} with respect to the corresponding e and μ asymmetries is not confirmed by the measurements of A_τ and Γ_τ which appear normal [1],[2],[7]. In principle the fact that an anomaly shows up in A_τ^{FB} and not in A_τ and Γ_τ is not unconceivable because the FB lepton asymmetries are very small and very precisely measured. For example, the extraction of A_τ^{FB} from the data on the angular distribution of τ 's could be biased if the imaginary part of the continuum was altered by some non universal new physics effect [8]. But a more trivial experimental problem is at the moment quite plausible.

A similar question can be asked for the b couplings. We have seen that the measured value of A_b^{FB} is about 2σ 's below the SM fit. At the same time R_b which used to show a major discrepancy is now only about 1.4σ 's away from the SM fit (as a result of the more sophisticated second generation experimental techniques). It is often stated that there is a -2.5σ deviation on the measured value of A_b vs the SM expectation [1],[2]. But in fact that depends on how the data are combined. In our opinion one should rather talk of a -1.8σ effect. Let us discuss this point in detail. A_b can be measured directly at SLC by taking advantage of the beam longitudinal polarization. At LEP one measures $A_b^{FB} = 3/4 A_e A_b$. One can then derive A_b by inserting a value for A_e . The question is what to use for A_e : the LEP value obtained,

Table 1: The electroweak data and the SM values obtained from a global fit.

Quantity	Data (August '97)	Standard Model Fit	Pull
m_Z (GeV)	91.1867(20)	91.1866	0.0
Γ_Z (GeV)	2.4948(25)	2.4966	-0.7
σ_h (nb)	41.486(53)	41.467	0.4
R_h	20.775(27)	20.756	0.7
R_b	0.2170(9)	0.2158	1.4
R_c	0.1734(48)	0.1723	-0.1
A_{FB}^l	0.0171(10)	0.0162	0.9
A_τ	0.1411(64)	0.1470	-0.9
A_e	0.1399(73)	0.1470	-1.0
A_{FB}^b	0.0983(24)	0.1031	-2.0
A_{FB}^c	0.0739(48)	0.0736	0.0
A_b (SLD direct)	0.900(50)	0.935	-0.7
A_c (SLD direct)	0.650(58)	0.668	-0.3
$\sin^2 \theta_{eff}$ (LEP-combined)	0.23199(28)	0.23152	1.7
$A_{LR} \rightarrow \sin^2 \theta_{eff}$	0.23055(41)	0.23152	-2.4
m_W (GeV) (LEP2+p \bar{p})	80.43(8)	80.375	0.7
$1 - \frac{m_W^2}{m_Z^2}$ (νN)	0.2254(37)	0.2231	0.6
Q_W (Atomic PV in Cs)	-72.11(93)	-73.20	1.2
m_t (GeV)	175.6(5.5)	173.1	0.4

using lepton universality, from the measurements of A_l^{FB} , A_τ , A_e : $A_e = 0.1461(33)$, or the combination of LEP and SLD etc. The LEP electroweak working group adopts for A_e the SLD+LEP average value which also includes A_{LR} from SLD: $A_e = 0.1505(23)$. This procedure leads to a -2.5σ deviation. However, in this case, the well known $\sim 2\sigma$ discrepancy of A_{LR} with respect to A_e measured at LEP and also to the SM fit, which is not related to the b couplings, further contributes to inflate the number of σ 's. Since we are here concerned with the b couplings it is perhaps wiser to obtain A_b from LEP by using the SM value for A_e (that is the pull-zero value of table 1): $A_e^{SM} = 0.1467(16)$. With the value of A_b derived in this way from LEP we finally obtain

$$A_b = 0.895 \pm 0.022 \quad (\text{LEP} + \text{SLD}, A_e = A_e^{\text{SM}} : -1.8) \quad (2)$$

In the SM A_b is so close to 1 because the b quark is almost purely left-handed. A_b only depends on the ratio $r = (g_R/g_L)^2$ which in the SM is small: $r \sim 0.033$. To adequately decrease A_b from its SM value one must increase r by a factor of about 1.6, which appears large for a new physics effect. Also such a large change in r must be compensated by decreasing g_L^2 by a small but fine-tuned amount in order to counterbalance the corresponding large positive shift in R_b . In view of this the most likely way out is that A_b^{FB} and A_b have been a bit underestimated at LEP and actually there is no anomaly in the b couplings. Then the LEP value of $\sin^2 \theta_{eff}$ would slightly move towards the SLD value, but, as explained above, by far not enough to remove the SLD-LEP discrepancy (for example, if the LEP average for $\sin^2 \theta_{eff}$ is computed by moving the central value of A_b^{FB} to the pull-zero value in table 1 with the same figure for the error, one finds $\sin^2 \theta_{eff} = 0.23162(28)$, a value still 2.2σ 's away from the SLD result).

3 Precision Electroweak Data and the Standard Model

For the analysis of electroweak data in the SM one starts from the input parameters: some of them, α , G_F and m_Z , are very well measured, some other ones, m_{flight} , m_t and $\alpha_s(m_Z)$ are only approximately determined while m_H is largely unknown. With respect to m_t the situation has much improved since the CDF/D0 direct measurement of the top quark mass [9]. From the input parameters one computes the radiative corrections [10] to a sufficient precision to match the experimental capabilities. Then one compares the theoretical predictions and the data for the numerous observables which have been measured, checks the consistency of the theory and derives constraints on m_t , $\alpha_s(m_Z)$ and hopefully also on m_H .

Some comments on the least known of the input parameters are now in order. The only practically relevant terms where precise values of the light quark masses, m_{flight} , are needed are those related to the hadronic contribution to the photon vacuum polarization diagrams, that determine $\alpha(m_Z)$. This correction is of order 6%, much larger than the accuracy of a few permil of the precision tests. Fortunately, one can use the actual data to in principle solve the related ambiguity. But the leftover uncertainty is still one of the main sources of theoretical error. In recent years there has been a lot of activity on this subject and a number of independent new estimates of $\alpha(m_Z)$ have appeared in the literature [11],(see also [12]). A consensus has been

Table 2: Measurements of $\alpha_s(m_Z)$. In parenthesis we indicate if the dominant source of errors is theoretical or experimental. For theoretical ambiguities our personal figure of merit is given.

Measurements	$\alpha_s(m_Z)$
R_τ	0.122 ± 0.006 (Th)
Deep Inelastic Scattering	0.116 ± 0.005 (Th)
Y_{decay}	0.112 ± 0.010 (Th)
Lattice QCD	0.117 ± 0.007 (Th)
$Re^+e^-(\sqrt{s} < 62 \text{ GeV})$	0.124 ± 0.021 (Exp)
Fragmentation functions in e^+e^-	0.124 ± 0.012 (Th)
Jets in e^+e^- at and below the Z	0.121 ± 0.008 (Th)
Z line shape (Assuming SM)	0.120 ± 0.004 (Exp)

established and the value used at present is

$$\alpha(m_Z)^{-1} = 128.90 \pm 0.09 \quad (3)$$

As for the strong coupling $\alpha_s(m_Z)$ the world average central value is by now quite stable. The error is going down because the dispersion among the different measurements is much smaller in the most recent set of data. The most important determinations of $\alpha_s(m_Z)$ are summarized in table 2 [13]. For all entries, the main sources of error are the theoretical ambiguities which are larger than the experimental errors. The only exception is the measurement from the electroweak precision tests, but only if one assumes that the SM electroweak sector is correct. Our personal views on the theoretical errors are reflected in the table 2. The error on the final average is taken by all authors between ± 0.003 and ± 0.005 depending on how conservative one is. Thus in the following our reference value will be

$$\alpha_s(m_Z) = 0.119 \pm 0.004 \quad (4)$$

Finally a few words on the current status of the direct measurement of m_t . The present combined CDF/D0 result is [9]

$$m_t = 175.6 \pm 5.5 \text{ GeV} \quad (5)$$

The error is so small by now that one is approaching a level where a more careful investigation of the effects of colour rearrangement on the determination of m_t is needed. One wants to determine the top quark mass, defined as the invariant mass of its decay products (i.e. $b+W+\text{gluons} + \gamma$'s). However, due to the need of colour rearrangement, the top quark and its decay products cannot be really isolated from the rest of the event. Some smearing of the mass distribution is induced by this colour crosstalk which involves the decay products of the top, those of the antitop and also the fragments of the incoming (anti)protons. A reliable quantitative computation of the smearing effect on the m_t determination is difficult because of the importance of non perturbative effects. An induced error of the order of one GeV on m_t is reasonably expected. Thus further progress on the m_t determination demands tackling this problem in more depth.

Table 3: Errors from different sources: Δ_{now}^{exp} is the present experimental error; $\Delta\alpha^{-1}$ is the impact of $\Delta\alpha^{-1} = \pm 0.09$; Δ_{th} is the estimated theoretical error from higher orders; Δm_t is from $\Delta m_t = \pm 6 \text{ GeV}$; Δm_H is from $\Delta m_H = 60\text{--}1000 \text{ GeV}$; $\Delta\alpha_s$ corresponds to $\Delta\alpha_s = \pm 0.003$. The epsilon parameters are defined in sect. 4.1 [18].

Parameter	Δ_{now}^{exp}	$\Delta\alpha^{-1}$	Δ_{th}	Δm_t	Δm_H	$\Delta\alpha_s$
Γ_Z (MeV)	± 2.5	± 0.7	± 0.8	± 1.4	± 4.6	± 1.7
σ_h (pb)	53	1	4.3	3.3	4	17
$R_h \cdot 10^3$	27	4.3	5	2	13.5	20
Γ_l (keV)	100	11	15	55	120	3.5
$A_{FB}^l \cdot 10^4$	10	4.2	1.3	3.3	13	0.18
$\sin^2\theta \cdot 10^4$	~ 3.2	2.3	0.8	1.9	7.5	0.1
m_W (MeV)	80	12	9	37	100	2.2
$R_b \cdot 10^4$	9	0.1	1	2.1	0.25	0
$\epsilon_1 \cdot 10^3$	1.2		~ 0.1			0.2
$\epsilon_3 \cdot 10^3$	1.4	0.5	~ 0.1			0.12
$\epsilon_b \cdot 10^3$	2.1		~ 0.1			1

In order to appreciate the relative importance of the different sources of theoretical errors for precision tests of the SM, we report in table 3 a comparison for the most relevant observables, evaluated using refs. [10],[14]. What is important to stress is that the ambiguity from m_t , once by far the largest one, is by now smaller than the error from m_H . We also see from table 3 that the error from $\Delta\alpha(m_Z)$ is especially important for $\sin^2\theta_{eff}$ and, to a lesser extent, is also sizeable for Γ_Z and ϵ_3 , to be defined later on.

The most important recent advance in the theory of radiative corrections is the calculation of the $o(g^4 m_t^2/m_W^2)$ terms in $\sin^2\theta_{eff}$ and m_W (not yet in $\delta\rho$) [15]. The result implies a small but visible correction to the predicted values but especially a sizeable decrease of the ambiguity from scheme dependence (a typical effect of truncation).

We now discuss fitting the data in the SM. Similar studies based on older sets of data are found in refs.[16]. As the mass of the top quark is finally rather precisely known from CDF and D0 one must distinguish two different types of fits. In one type one wants to answer the question: is m_t from radiative corrections in agreement with the direct measurement at the Tevatron? For answering this interesting but somewhat limited question, one must clearly exclude the CDF/D0 measurement of m_t from the input set of data. Fitting all other data in terms of m_t , m_H and $\alpha_s(m_Z)$ one finds the results shown in the third column of table 4 [2]. Other similar fits where also m_W direct data are left out are shown. The extracted value of m_t is typically a bit too low. There is a strong correlation between m_t and m_H . The results on $\sin^2\theta_{eff}$ and m_W [17] drive the fit to small values of m_H . This can be seen from figs.2 and 3 (note that in fig. 2 the value of $\sin^2\theta_{eff}$ found by SLD would be too low to be shown on the scale of the plot). Then, at small m_H , the widths drive the fit to small m_t (see fig. 4). In this context it is important to remark that fixing m_H at 300 GeV, as was often done in the past, is by now completely obsolete, because it introduces too strong a bias on the fitted value of m_t .

Table 4: SM fits from different sets of data (with and without the direct measurements of m_W and m_t).

Parameter	LEP(incl. m_W)	All but m_W, m_t	All but m_t	All Data
m_t (GeV)	158+14 – 11	157+10 – 9	161+10 – 8	173.1 ± 5.4
m_H (GeV)	83+168 – 49	41+64 – 21	42+75 – 23	115+116 – 66
$\log[m_H(\text{GeV})]$	1.92+0.48 – 0.39	1.62+0.41 – 0.31	1.63+0.44 – 0.33	2.06+0.30 – 0.37
$\alpha_s(m_Z)$	0.121 ± 0.003	0.120 ± 0.003	0.120 ± 0.003	0.120 ± 0.003
χ^2/dof	8/9	14/12	16/14	17/15

The change induced on the fitted value of m_t when moving m_H from 300 to 65 or 1000 GeV is in fact larger than the error on the direct measurement of m_t .

In a more general type of fit, e.g. for determining the overall consistency of the SM or the best present estimate for some quantity, say m_W , one should of course not ignore the existing direct determinations of m_t and m_W . Then, from all the available data, by fitting m_t , m_H and $\alpha_s(m_Z)$ one finds the values shown in the last column of table 4. This is the fit also referred to in table 1. The corresponding fitted values of $\sin^2 \theta_{eff}$ and m_W are:

$$\begin{aligned} \sin^2 \theta_{eff} &= 0.23152 \pm 0.00022, \\ m_W &= 80.375 \pm 0.030 \text{ GeV} \end{aligned} \tag{6}$$

The fitted value of $\sin^2 \theta_{eff}$ is identical to the LEP+SLD average and the caution on the error expressed in the previous section applies. The error of 30 MeV on m_W clearly sets up a goal for the direct measurement of m_W at LEP2 and the Tevatron.

As a final comment we want to recall that the radiative corrections are functions of $\log(m_H)$. It is truly remarkable that the fitted value of $\log(m_H)$ (the decimal logarithm) is found to fall right into the very narrow allowed window around the value 2 specified by the lower limit from direct searches, $m_H > 77$ GeV, and the theoretical upper limit in the SM $m_H < 600 - 800$ GeV (see sect.6). The fulfilment of this very stringent consistency check is a beautiful argument in favour of a fundamental Higgs (or one with a compositeness scale much above the weak scale).

4 A More General Analysis of Electroweak Data

We now discuss an update of the epsilon analysis [18] which is a method to look at the data in a more general context than the SM. The starting point is to isolate from the data that part which is due to the purely weak radiative corrections. In fact the epsilon variables are defined in such a way that they are zero in the approximation when only effects from the SM at tree level plus pure QED and pure QCD corrections are taken into account. This very simple version of improved Born approximation is a good first approximation according to the data and is independent of m_t and m_H . In fact the whole m_t and m_H dependence arises from weak loop corrections and therefore is only contained in the epsilon variables. Thus the epsilons are

extracted from the data without need of specifying m_t and m_H . But their predicted value in the SM or in any extension of it depend on m_t and m_H . This is to be compared with the competitor method based on the S, T, U variables [19],[20]. The latter cannot be obtained from the data without specifying m_t and m_H because they are defined as deviations from the complete SM prediction for specified m_t and m_H . Of course there are very many variables that vanish if pure weak loop corrections are neglected, at least one for each relevant observable. Thus for a useful definition we choose a set of representative observables that are used to parametrize those hot spots of the radiative corrections where new physics effects are most likely to show up. These sensitive weak correction terms include vacuum polarization diagrams which being potentially quadratically divergent are likely to contain all possible non decoupling effects (like the quadratic top quark mass dependence in the SM). There are three independent vacuum polarization contributions. In the same spirit, one must add the $Z \rightarrow b\bar{b}$ vertex which also includes a large top mass dependence. Thus altogether we consider four defining observables: one asymmetry, for example A_{FB}^l , (as representative of the set of measurements that lead to the determination of $\sin^2 \theta_{eff}$), one width (the leptonic width Γ_l is particularly suitable because it is practically independent of α_s), m_W and R_b . Here lepton universality has been taken for granted, because the data show that it is verified within the present accuracy. The four variables, ϵ_1 , ϵ_2 , ϵ_3 and ϵ_b are defined in ref.[18] in one to one correspondence with the set of observables A_l^{FB} , Γ_l , m_W , and R_b . The definition is so chosen that the quadratic top mass dependence is only present in ϵ_1 and ϵ_b , while the m_t dependence of ϵ_2 and ϵ_3 is logarithmic. The definition of ϵ_1 and ϵ_3 is specified in terms of A_l^{FB} and Γ_l only. Then adding m_W or R_b one obtains ϵ_2 or ϵ_b . We now specify the relevant definitions in detail.

4.1 Basic Definitions and Results

We start from the basic observables m_W/m_Z , Γ_l and A_l^{FB} and Γ_b . From these four quantities one can isolate the corresponding dynamically significant corrections Δr_W , $\Delta\rho$, Δk and ϵ_b , which contain the small effects one is trying to disentangle and are defined in the following. First we introduce Δr_W as obtained from m_W/m_Z by the relation:

$$\left(1 - \frac{m_W^2}{m_Z^2}\right) \frac{m_W^2}{m_Z^2} = \frac{\pi\alpha(m_Z)}{\sqrt{2}G_F m_Z^2 (1 - \Delta r_W)} \quad (7)$$

Here $\alpha(m_Z) = \alpha/(1 - \Delta\alpha)$ is fixed to the central value 1/128.90 so that the effect of the running of α due to known physics is extracted from $1 - \Delta r = (1 - \Delta\alpha)(1 - \Delta r_W)$. In fact, the error on $1/\alpha(m_Z)$, as given in eq.(3) would then affect Δr_W . In order to define $\Delta\rho$ and Δk we consider the effective vector and axial-vector couplings g_V and g_A of the on-shell Z to charged leptons, given by the formulae:

$$\Gamma_l = \frac{G_F m_Z^3}{6\pi\sqrt{2}} (g_V^2 + g_A^2) \left(1 + \frac{3\alpha}{4\pi}\right),$$

$$A_l^{FB}(\sqrt{s} = m_Z) = \frac{3g_V^2 g_A^2}{(g_V^2 + g_A^2)^2} = \frac{3x^2}{(1+x^2)^2}. \quad (8)$$

Note that Γ_l stands for the inclusive partial width $\Gamma(Z \rightarrow l\bar{l} + \text{photons})$. We stress the following points. First, we have extracted from $(g_V^2 + g_A^2)$ the factor $(1 + 3\alpha/4\pi)$ which is induced in Γ_l from final state radiation. Second, by the asymmetry at the peak in eq.(8) we mean the quantity which is commonly referred to by the LEP experiments (denoted as A_{FB}^0 in ref.[2]), which is corrected for all QED effects, including initial and final state radiation and also for the effect of the imaginary part of the γ vacuum polarization diagram. In terms of g_A and $x = g_V/g_A$, the quantities $\Delta\rho$ and Δk are given by:

$$\begin{aligned} g_A &= -\frac{\sqrt{\rho}}{2} \sim -\frac{1}{2}\left(1 + \frac{\Delta\rho}{2}\right), \\ x = \frac{g_V}{g_A} &= 1 - 4\sin^2\theta_{eff} = 1 - 4(1 + \Delta k)s_0^2. \end{aligned} \quad (9)$$

Here s_0^2 is $\sin^2\theta_{eff}$ before non pure-QED corrections, given by:

$$s_0^2 c_0^2 = \frac{\pi\alpha(m_Z)}{\sqrt{2}G_F m_Z^2} \quad (10)$$

with $c_0^2 = 1 - s_0^2$ ($s_0^2 = 0.231095$ for $m_Z = 91.188$ GeV).

We now define ϵ_b from Γ_b , the inclusive partial width for $Z \rightarrow b\bar{b}$ according to the relation

$$\Gamma_b = \frac{G_F m_Z^3}{6\pi\sqrt{2}} \beta \left(\frac{3 - \beta^2}{2} g_{bV}^2 + \beta^2 g_{bA}^2 \right) N_C R_{QCD} \left(1 + \frac{\alpha}{12\pi} \right) \quad (11)$$

where $N_C = 3$ is the number of colours, $\beta = \sqrt{1 - 4m_b^2/m_Z^2}$, with $m_b = 4.7$ GeV, R_{QCD} is the QCD correction factor given by

$$R_{QCD} = 1 + 1.2a - 1.1a^2 - 13a^3; \quad a = \frac{\alpha_s(m_Z)}{\pi} \quad (12)$$

and g_{bV} and g_{bA} are specified as follows

$$\begin{aligned} g_{bA} &= -\frac{1}{2}\left(1 + \frac{\Delta\rho}{2}\right)(1 + \epsilon_b), \\ \frac{g_{bV}}{g_{bA}} &= \frac{1 - 4/3\sin^2\theta_{eff} + \epsilon_b}{1 + \epsilon_b}. \end{aligned} \quad (13)$$

This is clearly not the most general deviation from the SM in the $Z \rightarrow b\bar{b}$ vertex but ϵ_b is closely related to the quantity $-Re(\delta_{b\text{-vertex}})$ defined in the last of refs.[21] where the large m_t corrections are located.

As is well known, in the SM the quantities Δr_W , $\Delta\rho$, Δk and ϵ_b , for sufficiently large m_t , are all dominated by quadratic terms in m_t of order $G_F m_t^2$. As new physics can more easily be disentangled if not masked by large conventional m_t effects, it is convenient to keep $\Delta\rho$ and ϵ_b while trading Δr_W and Δk for two quantities with no contributions of order $G_F m_t^2$. We thus introduce the following linear combinations:

$$\begin{aligned} \epsilon_1 &= \Delta\rho, \\ \epsilon_2 &= c_0^2 \Delta\rho + \frac{s_0^2 \Delta r_W}{c_0^2 - s_0^2} - 2s_0^2 \Delta k, \\ \epsilon_3 &= c_0^2 \Delta\rho + (c_0^2 - s_0^2) \Delta k. \end{aligned} \quad (14)$$

The quantities ϵ_2 and ϵ_3 no longer contain terms of order $G_F m_t^2$ but only logarithmic terms in m_t . The leading terms for large Higgs mass, which are logarithmic, are contained in ϵ_1 and ϵ_3 . In the Standard Model one has the following "large" asymptotic contributions:

$$\begin{aligned}
\epsilon_1 &= \frac{3G_F m_t^2}{8\pi^2 \sqrt{2}} - \frac{3G_F m_W^2}{4\pi^2 \sqrt{2}} \tan^2 \theta_W \ln \frac{m_H}{m_Z} + \dots, \\
\epsilon_2 &= -\frac{G_F m_W^2}{2\pi^2 \sqrt{2}} \ln \frac{m_t}{m_Z} + \dots, \\
\epsilon_3 &= \frac{G_F m_W^2}{12\pi^2 \sqrt{2}} \ln \frac{m_H}{m_Z} - \frac{G_F m_W^2}{6\pi^2 \sqrt{2}} \ln \frac{m_t}{m_Z} + \dots, \\
\epsilon_b &= -\frac{G_F m_t^2}{4\pi^2 \sqrt{2}} + \dots
\end{aligned} \tag{15}$$

The relations between the basic observables and the epsilons can be linearised, leading to the approximate formulae

$$\begin{aligned}
\frac{m_W^2}{m_Z^2} &= \frac{m_W^2}{m_Z^2}|_B (1 + 1.43\epsilon_1 - 1.00\epsilon_2 - 0.86\epsilon_3), \\
\Gamma_l &= \Gamma_l|_B (1 + 1.20\epsilon_1 - 0.26\epsilon_3), \\
A_l^{FB} &= A_l^{FB}|_B (1 + 34.72\epsilon_1 - 45.15\epsilon_3), \\
\Gamma_b &= \Gamma_b|_B (1 + 1.42\epsilon_1 - 0.54\epsilon_3 + 2.29\epsilon_b).
\end{aligned} \tag{16}$$

The Born approximations, as defined above, depend on $\alpha_s(m_Z)$ and also on $\alpha(m_Z)$. Defining

$$\delta\alpha_s = \frac{\alpha_s(m_Z) - 0.119}{\pi}; \quad \delta\alpha = \frac{\alpha(m_Z) - \frac{1}{128.90}}{\alpha}, \tag{17}$$

we have

$$\begin{aligned}
\frac{m_W^2}{m_Z^2}|_B &= 0.768905(1 - 0.40\delta\alpha), \\
\Gamma_l|_B &= 83.563(1 - 0.19\delta\alpha)\text{MeV}, \\
A_l^{FB}|_B &= 0.01696(1 - 34\delta\alpha), \\
\Gamma_b|_B &= 379.8(1 + 1.0\delta\alpha_s - 0.42\delta\alpha).
\end{aligned} \tag{18}$$

Note that the dependence on $\delta\alpha_s$ for $\Gamma_b|_B$, shown in eq.(18), is not simply the one loop result for $m_b = 0$ but a combined effective shift which takes into account both finite mass effects and the contribution of the known higher order terms.

The important property of the epsilons is that, in the Standard Model, for all observables at the Z pole, the whole dependence on m_t (and m_H) arising from one-loop diagrams only enters through the epsilons. The same is actually true, at the relevant level of precision, for all higher order m_t -dependent corrections. Actually, the only residual m_t dependence of the various observables not included in the epsilons is in the terms of order $\alpha_s^2(m_Z)$ in the pure QCD correction factors to the hadronic widths [22]. But this one is quantitatively irrelevant,

Table 5: Values of the epsilons in the SM as functions of m_t and m_H as obtained from recent versions[14] of ZFITTER and TOPAZ0 (also including the new results of ref.[15]). These values (in 10^{-3} units) are obtained for $\alpha_s(m_Z) = 0.119$, $\alpha(m_Z) = 1/128.90$, but the theoretical predictions are essentially independent of $\alpha_s(m_Z)$ and $\alpha(m_Z)$ [18].

m_t (GeV)	ϵ_1			ϵ_2			ϵ_3			ϵ_b All m_H
	m_H (GeV) =			m_H (GeV) =			m_H (GeV) =			
	70	300	1000	70	300	1000	70	300	1000	
150	3.55	2.86	1.72	-6.85	-6.46	-5.95	4.98	6.22	6.81	-4.50
160	4.37	3.66	2.50	-7.12	-6.72	-6.20	4.96	6.18	6.75	-5.31
170	5.26	4.52	3.32	-7.43	-7.01	-6.49	4.94	6.14	6.69	-6.17
180	6.19	5.42	4.18	-7.77	-7.35	-6.82	4.91	6.09	6.61	-7.08
190	7.18	6.35	5.09	-8.15	-7.75	-7.20	4.89	6.03	6.52	-8.03
200	8.22	7.34	6.04	-8.59	-8.18	-7.63	4.87	5.97	6.43	-9.01

especially in view of the errors connected to the uncertainty on the value of $\alpha_s(m_Z)$. The theoretical values of the epsilons in the SM from state of the art radiative corrections [10, 14], also including the recent development of ref.[15], are given in table 5. It is important to remark that the theoretical values of the epsilons in the SM, as given in table 2, are not affected, at the percent level or so, by reasonable variations of $\alpha_s(m_Z)$ and/or $\alpha(m_Z)$ around their central values. By our definitions, in fact, no terms of order $\alpha_s^n(m_Z)$ or $\alpha \ln m_Z/m$ contribute to the epsilons. In terms of the epsilons, the following expressions hold, within the SM, for the various precision observables

$$\begin{aligned}
\Gamma_T &= \Gamma_{T0}(1 + 1.35\epsilon_1 - 0.46\epsilon_3 + 0.35\epsilon_b), \\
R &= R_0(1 + 0.28\epsilon_1 - 0.36\epsilon_3 + 0.50\epsilon_b), \\
\sigma_h &= \sigma_{h0}(1 - 0.03\epsilon_1 + 0.04\epsilon_3 - 0.20\epsilon_b), \\
x &= x_0(1 + 17.6\epsilon_1 - 22.9\epsilon_3), \\
R_b &= R_{b0}(1 - 0.06\epsilon_1 + 0.07\epsilon_3 + 1.79\epsilon_b).
\end{aligned} \tag{19}$$

where $x=g_V/g_A$ as obtained from A_t^{FB} . The quantities in eqs.(16,19) are clearly not independent and the redundant information is reported for convenience. By comparison with the codes of ref.[14] (we also added the complete results of ref.[15]) we obtain

$$\begin{aligned}
\Gamma_{T0} &= 2489.46(1 + 0.73\delta\alpha_s - 0.35\delta\alpha) \text{ MeV}, \\
R_0 &= 20.8228(1 + 1.05\delta\alpha_s - 0.28\delta\alpha), \\
\sigma_{h0} &= 41.420(1 - 0.41\delta\alpha_s + 0.03\delta\alpha) \text{ nb}, \\
x_0 &= 0.075619 - 1.32\delta\alpha, \\
R_{b0} &= 0.2182355.
\end{aligned} \tag{20}$$

Note that the quantities in eqs.(20) should not be confused, at least in principle, with the corresponding Born approximations, due to small "non universal" electroweak corrections. In practice, at the relevant level of approximation, the difference between the two corresponding quantities is in any case significantly smaller than the present experimental error.

Table 6: Experimental values of the epsilons in the SM from different sets of data. These values (in 10^{-3} units) are obtained for $\alpha_s(m_Z) = 0.119 \pm 0.003$, $\alpha(m_Z) = 1/128.90 \pm 0.09$, the corresponding uncertainties being included in the quoted errors.

ϵ 10^3	Only def. quantities	All asymmetries	All High Energy	All Data
$\epsilon_1 10^3$	4.0 ± 1.2	4.3 ± 1.2	4.1 ± 1.2	3.9 ± 1.2
$\epsilon_2 10^3$	-8.3 ± 2.3	-9.1 ± 2.2	-9.3 ± 2.2	-9.4 ± 2.2
$\epsilon_3 10^3$	2.9 ± 1.9	4.3 ± 1.4	4.1 ± 1.4	3.9 ± 1.4
$\epsilon_b 10^3$	-3.2 ± 2.3	-3.3 ± 2.3	-3.9 ± 2.1	-3.9 ± 2.1

In principle, any four observables could have been picked up as defining variables. In practice we choose those that have a more clear physical significance and are more effective in the determination of the epsilons. In fact, since Γ_b is actually measured by R_b (which is nearly insensitive to α_s), it is preferable to use directly R_b itself as defining variable, as we shall do hereafter. In practice, since the value in eq.(20) is practically indistinguishable from the Born approximation of R_b , this determines no change in any of the equations given above but simply requires the corresponding replacement among the defining relations of the epsilons.

4.2 Experimental Determination of the Epsilon Variables

The values of the epsilons as obtained, following the specifications in the previous sect.4.1, from the defining variables m_W , Γ_l , A_l^{FB} and R_b are shown in the first column of table 6. To proceed further and include other measured observables in the analysis we need to make some dynamical assumptions. The minimum amount of model dependence is introduced by including other purely leptonic quantities at the Z pole such as A_τ , A_e (measured from the angular dependence of the τ polarization) and A_{LR} (measured by SLD). For this step, one is simply assuming that the different leptonic asymmetries are equivalent measurements of $\sin^2 \theta_{eff}$ (for an example of a peculiar model where this is not true, see ref.[23]). We add, as usual, the measure of A_b^{FB} because this observable is dominantly sensitive to the leptonic vertex. We then use the combined value of $\sin^2 \theta_{eff}$ obtained from the whole set of asymmetries measured at LEP and SLC with the error increased according to eq.(1) and the related discussion. At this stage the best values of the epsilons are shown in the second column of table 6. In figs. 5-8 we report the 1σ ellipses in the indicated ϵ_i - ϵ_j planes that correspond to this set of input data. In fig. 9, for example, we also give a graphical representation in the ϵ_3 - ϵ_b plane, of the uncertainties due to $\alpha(m_Z)$ and $\alpha_s(m_Z)$.

All observables measured on the Z peak at LEP can be included in the analysis provided that we assume that all deviations from the SM are only contained in vacuum polarization diagrams (without demanding a truncation of the q^2 dependence of the corresponding functions) and/or the $Z \rightarrow b\bar{b}$ vertex. From a global fit of the data on m_W , Γ_T , R_h , σ_h , R_b and $\sin^2 \theta_{eff}$ (for LEP data, we have taken the correlation matrix for Γ_T , R_h and σ_h given by the LEP experiments [2], while we have considered the additional information on R_b and $\sin^2 \theta_{eff}$ as independent) we obtain the values shown in the third column of table 6. The comparison of theory and experiment at this stage is also shown in figs. 5-8. More detailed information is shown in figs.

10-11, which both refer to the level when also hadronic data are taken into account. But in fig. 10 we compare the results obtained if $\sin^2 \theta_{eff}$ is extracted in turn from different asymmetries among those listed in fig. 1. The ellipse marked "average" is the same as the one labeled "All high en." in fig. 6 and corresponds to the value of $\sin^2 \theta_{eff}$ which is shown on the figure (and in eq.(1)). We confirm that the value from A_{LR} is far away from the SM given the experimental value of m_t and the bounds on m_H and would correspond to very small values of ϵ_3 and of ϵ_1 . We see also that while the τ FB asymmetry is also on the low side, the combined e and μ FB asymmetry are right on top of the average. Finally the b FB asymmetry is on the high side. An analogous plot is presented in fig. 11. In this case the defining width Γ_l is replaced in turn with either the total or the hadronic or the invisible width. The important conclusion that one obtains is that the widths are indeed well consistent among them even with respect to this new criterium of leading to the same epsilons.

To include in our analysis lower energy observables as well, a stronger hypothesis needs to be made: vacuum polarization diagrams are allowed to vary from the SM only in their constant and first derivative terms in a q^2 expansion [19]-[20]. In such a case, one can, for example, add to the analysis the ratio R_ν of neutral to charged current processes in deep inelastic neutrino scattering on nuclei [24], the "weak charge" Q_W measured in atomic parity violation experiments on Cs [25] and the measurement of g_V/g_A from $\nu_\mu e$ scattering [26]. In this way one obtains the global fit given in the fourth column of table 6 and shown in figs. 5-8. For completeness, we also report the corresponding values of Δr_W and Δk (defined in eqs. (7,9)): $10^3 \times \Delta r_W = -27.0 \pm 4.3$, $10^3 \times \Delta k = 16.7 \pm 18.4$. With the progress of LEP the low energy data, while important as a check that no deviations from the expected q^2 dependence arise, play a lesser role in the global fit. Note that the present ambiguity on the value of $\delta\alpha^{-1}(m_Z) = \pm 0.09$ [11] corresponds to an uncertainty on ϵ_3 (the other epsilons are not much affected) given by $\Delta\epsilon_3 10^3 = \pm 0.6$ [18]. Thus the theoretical error is still comfortably less than the experimental error. In fig. 12 we present a summary of the experimental values of the epsilons as compared to the SM predictions as functions of m_t and m_H , which shows agreement within 1σ . However the central values of ϵ_1 , ϵ_2 and ϵ_3 are all somewhat low, while the central value of ϵ_b is shifted upward with respect to the SM as a consequence of the still imperfect matching of R_b .

A number of interesting features are clearly visible from figs.5-12. First, the good agreement with the SM and the evidence for weak corrections, measured by the distance of the data from the improved Born approximation point (based on tree level SM plus pure QED or QCD corrections). There is by now a solid evidence for departures from the improved Born approximation where all the epsilons vanish. In other words a clear evidence for the pure weak radiative corrections has been obtained and LEP/SLC are now measuring the various components of these radiative corrections. For example, some authors [27] have studied the sensitivity of the data to a particularly interesting subset of the weak radiative corrections, i.e. the purely bosonic part. These terms arise from virtual exchange of gauge bosons and Higgses. The result is that indeed the measurements are sufficiently precise to require the presence of these contributions in order to fit the data. Second, the general results of the SM fits are reobtained from a different perspective. We see the preference for light Higgs manifested by the tendency for ϵ_3 to be rather on the low side. Since ϵ_3 is practically independent of m_t , its low value demands m_H small. If the Higgs is light then the preferred value of m_t is somewhat lower than the Tevatron

result (which in the epsilon analysis is not included among the input data). This is because also the value of $\epsilon_1 \equiv \delta\rho$, which is determined by the widths, in particular by the leptonic width, is somewhat low. In fact ϵ_1 increases with m_t and, at fixed m_t , decreases with m_H , so that for small m_H the low central value of ϵ_1 pushes m_t down. Note that also the central value of ϵ_2 is on the low side, because the experimental value of m_W is a little bit too large. Finally, we see that adding the hadronic quantities or the low energy observables hardly makes a difference in the ϵ_i - ϵ_j plots with respect to the case with only the leptonic variables being included (the ellipse denoted by "All Asymm."). But, take for example the ϵ_1 - ϵ_3 plot: while the leptonic ellipse contains the same information as one could obtain from a $\sin^2\theta_{eff}$ vs Γ_l plot, the content of the other two ellipses is much larger because it shows that the hadronic as well as the low energy quantities match the leptonic variables without need of any new physics. Note that the experimental values of ϵ_1 and ϵ_3 when the hadronic quantities are included also depend on the input value of α_s given in eq.(4).

4.3 Comparing the Data with the Minimal Supersymmetric Standard Model

The MSSM [28] is a completely specified, consistent and computable theory. There are too many parameters to attempt a direct fit of the data to the most general framework. So we consider two significant limiting cases: the "heavy" and the "light" MSSM.

The "heavy" limit corresponds to all sparticles being sufficiently massive, still within the limits of a natural explanation of the weak scale of mass. In this limit a very important result holds [29]: for what concerns the precision electroweak tests, the MSSM predictions tend to reproduce the results of the SM with a light Higgs, say $m_H \sim 100$ GeV. So if the masses of SUSY partners are pushed at sufficiently large values the same quality of fit as for the SM is guaranteed. Note that for $m_t = 175.6$ GeV and $m_H \sim 70$ GeV the values of the four epsilons computed in the SM lead to a fit of the corresponding experimental values with $\chi^2 \sim 4$, which is reasonable for $d.o.f = 4$. This value corresponds to the fact that the central values of $\epsilon_1, \epsilon_2, \epsilon_3$ and $-\epsilon_b$ are all below the SM value by about 1σ , as can be seen from fig. 12.

In the "light" MSSM option some of the superpartners have a relatively small mass, close to their experimental lower bounds. In this case the pattern of radiative corrections may sizeably deviate from that of the SM [30]. The potentially largest effects occur in vacuum polarisation amplitudes and/or the $Z \rightarrow b\bar{b}$ vertex. In particular we recall the following contributions :

i) a threshold effect in the Z wave function renormalisation [29] mostly due to the vector coupling of charginos and (off-diagonal) neutralinos to the Z itself. Defining the vacuum polarisation functions by $\Pi_{\mu\nu}(q^2) = -ig_{\mu\nu}[A(0) + q^2 F(q^2)] + q_\mu q_\nu$ terms, this is a positive contribution to $\epsilon_5 = m_Z^2 F'_{ZZ}(m_Z^2)$, the prime denoting a derivative with respect to q^2 (i.e. a contribution to a higher derivative term not included in the naive epsilon formalism, but compatible with the scheme described in Sect. 4.1). The ϵ_5 correction shifts ϵ_1, ϵ_2 and ϵ_3 by $-\epsilon_5, -c^2\epsilon_5$ and $-c^2\epsilon_5$ respectively, where $c^2 = \cos^2\theta_W$, so that all of them are reduced by a comparable amount. Correspondingly all the Z widths are reduced without affecting the asymmetries. This effect

falls down particularly fast when the lightest chargino mass increases from a value close to $m_Z/2$. Now that we know, from the LEP2 runs, that the chargino mass is probably not smaller than m_Z its possible impact is drastically reduced.

ii) a positive contribution to ϵ_1 from the virtual exchange of split multiplets of SUSY partners, for example of the scalar top and bottom superpartners [31], analogous to the contribution of the top-bottom left-handed quark doublet. From the experimental value of m_t not much space is left for this possibility, and the experimental value of ϵ_1 is an important constraint on the spectrum. This is especially true now that the rather large lower limits on the chargino mass reduce the size of a possible compensation from ϵ_5 . For example, if the stop is light then it must be mainly a right-handed stop. Also large values of $\tan\beta$ are disfavoured because they tend to enhance the splittings among SUSY partner multiplets. In general it is simpler to decrease the predicted values of ϵ_2 and ϵ_3 by taking advantage of ϵ_5 than to decrease ϵ_1 , because the negative shift from ϵ_5 is most often counterbalanced by the increase from the effect of split SUSY multiplets.

iii) a negative contribution to ϵ_b due to the virtual exchange of a charged Higgs [32]. If one defines, as customary, $\tan\beta = v_2/v_1$ (v_1 and v_2 being the vacuum expectation values of the Higgs doublets giving masses to the down and up quarks, respectively), then, for negligible bottom Yukawa coupling or $\tan\beta \ll m_t/m_b$, this contribution is proportional to $m_t^2/\tan^2\beta$.

iv) a positive contribution to ϵ_b due to virtual chargino–stop exchange [33] which in this case is proportional to $m_t^2/\sin^2\beta$ and prefers small $\tan\beta$. This effect again requires the chargino and the stop to be light in order to be sizeable.

With the recent limits set by LEP2 on the masses of SUSY partners the above effects are small enough that other contributions from vertex diagrams could be comparable. Thus in the following we will only consider the experimental values of the epsilons obtained at the level denoted by "All Asymmetries" which only assumes lepton universality.

We have analysed the problem of what configurations of masses in the "light" MSSM are favoured or disfavoured by the present data (updating ref.[34]). We find that no lower limits on the masses of SUSY partners are obtained which are better than the direct limits. One exception is the case of stop and sbottom masses, which are severely constrained by the ϵ_1 value and also, at small $\tan\beta$, by the increase at LEP2 of the direct limit on the Higgs mass. Charged Higgs masses are also constrained. Since the central values of ϵ_1, ϵ_2 and ϵ_3 are all below the SM it is convenient to make ϵ_5 as large as possible. For this purpose light gaugino and slepton masses are favoured. We find that for $m_{\chi_1^\pm} \sim 90 - 120$ GeV the effect is still sizeable. Also favoured are small values of $\tan\beta$ that allow to put slepton masses relatively low, say, in the range 100-500 GeV, without making the split in the isospin doublets too large for ϵ_1 . Charged Higgses must be heavy because they contribute to ϵ_b with the wrong sign. A light right-handed stop could help on R_b for a Higgsino-like chargino. But one needs small mixing (the right-handed stop must be close to the mass eigenstate) and beware of the Higgs mass constraint at small $\tan\beta$ (a Higgs mass above ~ 80 GeV, the range of LEP2 for susy Higgses at $\sqrt{s} = 183$ GeV, starts being a strong constraint at small $\tan\beta$). So we prefer in the following to keep the stop mass large. The limits on $b \rightarrow s\gamma$ also prefer heavy charged Higgs and stop

[35].

The scatter plots obtained in the planes ϵ_1 - ϵ_3 and ϵ_2 - ϵ_3 for $-200 < \mu < 200$ GeV, $0 < M < 250$ GeV, $\tan \beta = 1.5 - 2.5$, $m_{\tilde{l}} = 100 - 500$ GeV and $m_{\tilde{q}} = 1$ TeV are shown in figs. 13 and 14, together with the SM prediction for $m_t = 175.6$ GeV and $m_h \sim 70$ GeV. We see that in most cases the χ^2 is not improved. If we restrict to the small area, marked with a small star in fig. 13, where both ϵ_1 and ϵ_3 are improved we can check that also ϵ_2 is improved, as is seen from fig. 14 where the same values of the parameters have been employed in the region marked with the star. This region where the χ^2 is decreased by slightly more than one unity is included in the hypervolume $\mu = 133 - 147$ GeV, $M = 212 - 250$ GeV, ($m_{\chi_1^+} = 90 - 105$ GeV, $m_{\chi_1^0} = 58 - 72$ GeV, $m_{\chi_2^0} = 129 - 147$ GeV) with $\tan \beta \sim 1.5$, $m_{\tilde{q}} \sim 1$ TeV and $m_{\tilde{l}} = 100$ GeV. In this configuration ϵ_b is unchanged. We see that the advantage with respect to the SM is at most of the order of 1 in χ^2 .

5 Theoretical Limits on the Higgs Mass

The SM works with remarkable accuracy. But the experimental foundation of the SM is not completed if the electroweak symmetry breaking mechanism is not experimentally established. Experiments must decide what is true: the SM Higgs or Higgs plus SUSY or new strong forces and Higgs compositeness.

The theoretical limits on the Higgs mass play an important role in the planning of the experimental strategy. The large experimental value of m_t has important implications on m_H both in the minimal SM [36]–[38] and in its minimal supersymmetric extension[39],[40].

It is well known[36]–[38] that in the SM with only one Higgs doublet a lower limit on m_H can be derived from the requirement of vacuum stability. The limit is a function of m_t and of the energy scale Λ where the model breaks down and new physics appears. Similarly an upper bound on m_H (with mild dependence on m_t) is obtained [41] from the requirement that up to the scale Λ no Landau pole appears. If one demands vacuum stability up to a very large scale, of the order of M_{GUT} or M_{Pl} then the resulting bound on m_H in the SM with only one Higgs doublet is given by [37]:

$$m_H(\text{GeV}) > 138 + 2.1 [m_t(\text{GeV}) - 175.6] - 3.0 \frac{\alpha_s(m_Z) - 0.119}{0.004}. \quad (21)$$

In fact one can show that the discovery of a Higgs particle at LEP2, or $m_H \lesssim 100$ GeV, would imply that the SM breaks down at a scale Λ of the order of a few TeV. Of course, the limit is only valid in the SM with one doublet of Higgses. It is enough to add a second doublet to avoid the lower limit. The upper limit on the Higgs mass in the SM is important for assessing the chances of success of the LHC as an accelerator designed to solve the Higgs problem. The upper limit [41] has been recently reevaluated [42]. For $m_t \sim 175$ GeV one finds $m_H \lesssim 180$ GeV for $\Lambda \sim M_{GUT} - M_{Pl}$ and $m_H \lesssim 0.5 - 0.8$ TeV for $\Lambda \sim 1$ TeV.

A particularly important example of a theory where the bound is violated is the MSSM,

which we now discuss. As is well known [28], in the MSSM there are two Higgs doublets, which implies three neutral physical Higgs particles and a pair of charged Higgses. The lightest neutral Higgs, called h , should be lighter than m_Z at tree-level approximation. However, radiative corrections [43] increase the h mass by a term proportional to m_t^4 and logarithmically dependent on the stop mass. Once the radiative corrections are taken into account the h mass still remains rather small: for $m_t = 174$ GeV one finds the limit (for all values of $\tan\beta$) $m_h < 130$ GeV [40]. Actually there are reasons to expect that m_h is well below the bound. In fact, if h_t is large at the GUT scale, which is suggested by the large observed value of m_t and by a natural onset of the electroweak symmetry breaking induced by m_t , then at low energy a fixed point is reached in the evolution of m_t . The fixed point corresponds to $m_t \sim 195 \sin\beta$ GeV (a good approximate relation for $\tan\beta = v_{up}/v_{down} < 10$). If the fixed point situation is realized, then m_h is considerably below the bound, $m_h \lesssim 100$ GeV [40].

In conclusion, for $m_t \sim 175$ GeV, we have seen that, on the one hand, if a Higgs is found at LEP the SM cannot be valid up to M_{Pl} . On the other hand, if a Higgs is found at LEP, then the MSSM has good chances, because this model would be excluded for $m_h > 130$ GeV.

6 Conclusion

The experiments performed in recent years mainly at LEP but also at SLAC and at the Tevatron have allowed to test the SM of the electroweak interactions with unprecedented precision. A number of observables measured at the per mille level can be successfully fitted in terms of the most relevant parameters of the SM, m_t , $\alpha_S(m_Z)$ and m_H . The presence of a few $\sim 2\sigma$ deviations is what is to be expected on statistical grounds. Furthermore, a closer look at such deviations does not give any hint of a significant pattern. An annoying feature of the data is the persistent difference between the values of $\sin^2\theta_{eff}$ measured at LEP and at SLC. There are reasons to think, however, that this difference will be understood by the further data-taking at SLAC and by the completion of the LEP analyses of the τ and b asymmetries.

A way to appreciate the significance of the attained precision is to notice, as shown in table 3, that the uncertainties on most of the observables are dominated, in the SM, by the variation of the Higgs mass from 60 to 1000 GeV and that such effect is often larger than the experimental error. Remarkably, the fitted value of $\log(m_H)$, which gets fixed in this way, falls right on top of the range specified by the experimental lower limit and the theoretical upper bound. We interpret this as indirect evidence for a weakly interacting Higgs, or Higgs plus SUSY, against new strong forces or an Higgs composite at a light scale. This is a clear and easier conclusion than setting an upper bound on the Higgs mass, within the SM, relevant to its search in different machines, LEP, Tevatron or LHC. In this respect, it is only unfortunate that $\sin^2\theta_{eff}$, which is among the most sensitive observables, suffers of the problem pointed out before. In turn, this emphasizes the importance of the direct measurement of m_W at LEP2 and the Tevatron, again because of its sensitivity to the Higgs mass.

The analysis of the data in terms of the epsilon parameters shows the significance of the

precision tests in a more general context than the SM itself. It would be most useful in the case that deviations were put in evidence. This not being the case, this analysis serves mostly to illustrate the evidence reached for quantum electroweak effects. In the space of the ϵ parameters the region indicated by the data clearly excludes the Born point, i.e. the origin, by many σ 's. Since these parameters are successfully fitted in the SM, any extension, or alternative of it must be delicate enough not to undo this agreement. This is the case for the MSSM, as clearly illustrated in fig.s 13, 14. For what concerns the precision electroweak tests, the MSSM predictions reproduce the SM with a light Higgs as soon as the sparticle masses are sufficiently heavy, but still compatible with the naturalness bound. A marginal reduction of the χ^2 is possible in a small region of the MSSM parameter space, to which we cannot attach, however, at the moment any particular significance.

FIGURE CAPTIONS

1. The collected measurements of $\sin^2\theta_{eff}$. The resulting value for the χ^2 is given by $\chi^2/d.o.f = 1.87$. As a consequence the error on the average is enlarged in the text by a factor $\sqrt{1.87}$ with respect to the formal average shown here.

2. SM prediction for $\sin^2\theta_{eff}$ as function of m_H for $m_t = 175.6 \pm 5.5$ as computed from updated radiative corrections [15]. The theoretical error bands from neglect of higher order terms, estimated from scheme and scale dependence, are shown. The combined LEP+SLD experimental value is indicatively plotted for $m_H \sim 100$ GeV (the SLD value would be very low, out of the plot scale). Small values of m_H are preferred.

3. SM prediction for m_W as function of m_H for $m_t = 175.6 \pm 5.5$ as computed from updated radiative corrections [15]. The theoretical error bands from neglect of higher order terms, estimated from scheme and scale dependence, are shown. The combined LEP+hadron colliders experimental value is indicatively plotted for $m_H \sim 100$ GeV. Small values of m_H are preferred.

4. SM prediction for the leptonic width as function of m_t . For small Higgs mass a value of m_t slightly smaller than the CDF/D0 experimental value is indicated.

5. Data vs theory in the ϵ_2 - ϵ_1 plane. The origin point corresponds to the "Born" approximation obtained from the SM at tree level plus pure QED and pure QCD corrections. The predictions of the full SM (also including the improvements of ref.[15]) are shown for $m_H = 70, 300$ and 1000 GeV and $m_t = 175.6 \pm 5.5$ GeV (a segment for each m_H with the arrow showing the direction of m_t increasing from $-\sigma$ to $+\sigma$). The three $1 - \sigma$ ellipses (38% probability contours) are obtained from a) "All Asymm.": Γ_l, m_W and $\sin^2\theta_{eff}$ as obtained from the combined asymmetries (the value and error used are shown); b) "All High En.": the same as in a) plus all the hadronic variables at the Z; c) "All Data": the same as in b) plus the low energy data.

6. Data vs theory in the ϵ_3 - ϵ_1 plane (notations as in fig. 5).

7. Data vs theory in the ϵ_2 - ϵ_3 plane (notations as in fig. 5).

8. Data vs theory in the ϵ_b - ϵ_1 plane (notations as in fig. 5).

9. Data vs theory in the ϵ_3 - ϵ_b plane (notations as in fig. 5, except that both ellipses refer to the case b)) The inner $1 - \sigma$ ellipse is without the errors induced by the uncertainties on $\alpha(m_Z)$ and $\alpha_s(m_Z)$.

10. Data vs theory in the ϵ_3 - ϵ_1 plane (notations as in fig. 5). The ellipse indicated with "Average" corresponds to the case "All high en" of fig. 6 and is obtained from the average value of $\sin^2\theta_{eff}$ displayed on the figure. The other ellipses are obtained by replacing the average $\sin^2\theta_{eff}$ with the values obtained in turn from each individual asymmetry as shown by the labels.

11. Data vs theory in the ϵ_3 - ϵ_1 plane (notations as in fig. 5). The different ellipses are obtained from m_W , the average value of $\sin^2\theta_{eff}$ displayed on the figure, R_b plus one width among Γ_l , Γ_{inv} , the total width Γ_Z and Γ_h .

12. The bands (labeled by the ϵ index) are the predicted values of the epsilons in the SM as functions of m_t for $m_H = 70 - 1000$ GeV (the m_H value corresponding to one edge of the band is indicated). The CDF/D0 experimental $1-\sigma$ range of m_t is shown. The experimental results for the epsilons from all data are displayed (from the last column of table 6). The position of the data on the m_t axis has been arbitrarily chosen and has no particular meaning.

13. Scatter plot obtained in the plane ϵ_1 - ϵ_3 for $-200 < \mu < 200$ GeV, $0 < M < 250$ GeV, $\tan\beta = 1.5 - 2.5$, $m_{\tilde{l}} = 100 - 500$ GeV and $m_{\tilde{q}} = 1$ TeV, together with the SM prediction for $m_t = 175.6$ GeV and $m_H \sim 70$ GeV. The separation $\mu > 0$ or $\mu < 0$ is clearly visible. The small star indicates the region with minimum χ^2 .

14. Scatter plot obtained in the plane ϵ_2 - ϵ_3 for $-200 < \mu < 200$ GeV, $0 < M < 250$ GeV, $\tan\beta = 1.5 - 2.5$, $m_{\tilde{l}} = 100 - 500$ GeV and $m_{\tilde{q}} = 1$ TeV, together with the SM prediction for $m_t = 175.6$ GeV and $m_H \sim 70$ GeV. The small star corresponds to the same values of the parameters of the region (marked with a star) in fig. 13. For these values of parameters the fit of ϵ_1, ϵ_2 and ϵ_3 improves while ϵ_b is unchanged.

References

- [1] J.Timmermans, Proceedings of LP'97, Hamburg, 1997; S. Dong, ibidem; D.Ward, Proceedings of HEP97, Jerusalem, 1997.
- [2] The LEP Electroweak Working Group, LEPEWWG/97-02.
- [3] C.Dionisi, Proceedings of LP'97, Hamburg, 1997; P.Janot, Proceedings of HEP97, Jerusalem, 1997.
- [4] S. Weinberg, Phys. Rev. D13(1976)974 and Phys. Rev. D19(1979)1277; L. Susskind, Phys. Rev. D20(1979)2619; E. Farhi and L. Susskind, Phys. Rep. 74(1981)277.
- [5] R. Casalbuoni et al., Phys. Lett. B258(1991)161; R.N. Cahn and M. Suzuki, LBL-30351 (1991); C. Roisnel and Tran N. Truong, Phys. Lett. B253(1991)439; T. Appelquist and G.

- Triantaphyllou, Phys. Lett. B278(1992)345; T. Appelquist, Proceedings of the Rencontres de la Valle d'Aoste, La Thuile, Italy, 1993; R.Chivukula, hep-ph/9701322.
- [6] J. Ellis, G.L. Fogli and E. Lisi, Phys. Lett. B343(1995)282.
- [7] W.Li, Proceedings of LP'97, Hamburg, 1997.
- [8] F.Caravaglios, Phys.Lett.B394(1997)359.
- [9] P.Giromini, Proceedings of LP'97, Hamburg, 1997; A. Yagil, Proceedings of HEP97, Jerusalem, 1997.
- [10] G. Altarelli, R. Kleiss and C. Verzegnassi (eds.), Z Physics at LEP 1 (CERN 89- 08, Geneva, 1989), Vols. 1-3; Precision Calculations for the Z Resonance, ed. by D.Bardin, W.Hollik and G.Passarino, CERN Rep 95-03 (1995); M.I. Vysotskii, V.A. Novikov, L.B. Okun and A.N. Rozanov, hep-ph/9606253.
- [11] F.Jegerlehner, Z.Phys. C32(1986)195, B.W.Lynn, G.Penso and C.Verzegnassi, Phys.Rev. D35(1987)42; H.Burkhardt et al., Z.Phys. C43(1989)497; F.Jegerlehner, Progr. Part. Nucl. Phys. 27(1991)32; M.L.Swartz, Preprint SLAC-PUB-6710, 1994; M.L.Swartz, Phys.Rev.D53(1996)5268; A.D.Martin and D.Zeppenfeld, Phys.Letters B345(1995)558; R.B. Nevzorov, A.V. Novikov, M.I. Vysotskii, hep-ph/9405390; H.Burkhardt and B.Pietrzyk, Phys. Lett. B356(1995)398; S.Eidelman and F.Jegerlehner, Z.Phys. C67(1995)585.
- [12] B.Pietrzyk, Proceedings of the Symposium on Radiative Corrections, Cracow, 1996.
- [13] S.Catani, Proceedings of LP'97, Hamburg, 1997; Yu.L. Dokshitser, Proceedings of HEP97, Jerusalem, 1997.
- [14] ZFITTER: D. Bardin et al., CERN-TH. 6443/92 and refs. therein; TOPAZ0: G. Montagna et al., Nucl. Phys. B401(1993)3, Comp. Phys. Comm. 76(1993)328; BHM: G.Burgers et al., LEPTOP: A.V. Novikov, L.B.Okun and M.I. Vysotsky, Mod.Phys.Lett.A8(1993)2529; WOH, W.Hollik : see ref. [10].
- [15] G.Degrassi, P.Gambino and A.Vicini, Phys. Lett. B383(1996)219; G.Degrassi, P.Gambino and A.Sirlin, Phys. Lett. B394(1997)188; G.Degrassi, P.Gambino, M.Passera and A.Sirlin, hep-ph/9708311.
- [16] J. Ellis, G.L. Fogli and E. Lisi, Phys. Lett. B389(1996)321; G.Altarelli, hep-ph/9611239; A.Gurtu, Phys. Lett. B385(1996)415; P.Langacker and J.Erler, hep-ph/9703428; J.L.Rosner, hep-ph/9704331; K.Hagiwara, D.Haidt and S.Matsumoto, hep-ph/9706331.
- [17] Y.Y.Kim, Proceedings of LP'97, Hamburg, 1997.
- [18] G. Altarelli, R. Barbieri and S. Jadach, Nucl. Phys. B369(1992)3; G. Altarelli, R. Barbieri and F. Caravaglios, Nucl. Phys. B405(1993)3; Phys. Lett. B349(1995)145.
- [19] M.E. Peskin and T. Takeuchi, Phys. Rev. Lett. 65(1990)964 and Phys. Rev. D46(1991)381.

- [20] G. Altarelli and R. Barbieri, Phys. Lett. B253(1990)161; B.W. Lynn, M.E. Peskin and R.G. Stuart, SLAC-PUB-3725 (1985); in Physics at LEP, Yellow Book CERN 86-02, Vol. I, p. 90; B. Holdom and J. Terning, Phys. Lett. B247(1990)88; D.C. Kennedy and P. Langacker, Phys. Rev. Lett. 65(1990)2967.
- [21] A.A. Akundov et al., Nucl. Phys. B276(1988)1; F. Diakonov and W. Wetzel, HD-THEP-88-4 (1988); W. Beenakker and H. Hollik, Z. Phys. C40(1988)569; B.W. Lynn and R.G. Stuart, Phys. Lett. B252(1990)676; J. Bernabeu, A. Pich and A. Santamaria, Phys. Lett. B200(1988)569; Nucl. Phys. B363(1991)326.
- [22] B.A.Kniehl and J.H.Kuhn, Phys. Lett. B224(1989)229; Nucl.Phys. B329(1990)547.
- [23] F. Caravaglios and G.G.Ross, Phys. Lett. B346(1995)159.
- [24] CHARM Collaboration, J.V. Allaby et al., Phys. Lett. B177(1986)446; Z. Phys. C36(1987)611; CDHS Collaboration, H. Abramowicz et al., Phys. Rev. Lett. 57(1986)298; A. Blondel et al., Z. Phys. C45 (1990) 361; CCFR Collaboration, K.McFarland, hep-ex/9701010.
- [25] C.S.Wood et al., Science 275(1997)1759.
- [26] CHARM II Collaboration, P.Vilain et al., Phys. Lett. B335(1997)246.
- [27] S. Dittmaier, D. Schildknecht, K. Kolodziej, M. Kuroda Nucl. Phys. B426(1994)249; B446(1995)334; A. Sirlin, and P. Gambino, Phys. Rev. Lett. 73(1994)621; S. Dittmaier, D. Schildknecht and G.Weiglein, Nucl. Phys. B465(1996)3.
- [28] H.P. Nilles, Phys. Rep. C110(1984)1;
H.E. Haber and G.L. Kane, Phys. Rep. C117(1985)75;
R. Barbieri, Riv. Nuovo Cim. 11(1988)1.
- [29] R. Barbieri, F. Caravaglios and M. Frigeni, Phys. Lett. B279(1992)169.
- [30] S.Pokorski, Proceedings of ICHEP'96, Warsaw, 1996; see also P. Chankowski, J. Ellis and S. Pokorski, CERN preprint TH/97-343, hep-ph/9712234.
- [31] R. Barbieri and L. Maiani, Nucl. Phys. B224(1983)32;
L. Alvarez-Gaumé, J. Polchinski and M. Wise, Nucl. Phys. B221(1983)495.
- [32] W. Hollik, Mod. Phys. Lett. A5(1990)1909.
- [33] A. Djouadi et al., Nucl. Phys. B349(1991)48;
M. Boulware and D. Finnell, Phys. Rev. D44(1991)2054. The sign discrepancy between these two papers appears now to be solved in favour of the second one.
- [34] G. Altarelli, R. Barbieri and F. Caravaglios, Phys. Lett. B314(1993)357.
- [35] A. Brignole, F. Feruglio and F. Zwirner Z. Phys. C71(1996)679.

- [36] M. Sher, Phys. Rep. 179(1989)273; Phys. Lett. B317(1993)159.
- [37] G. Altarelli and G. Isidori, Phys. Lett. B337(1994)141.
- [38] J.A. Casas, J.R. Espinosa and M. Quiros, Phys. Lett. B342(1995)171.
- [39] J.A. Casas et al., Nucl. Phys. B436(1995)3; E B439(1995)466.
- [40] M. Carena and C.E.M. Wagner, Nucl. Phys. B452(1995)45.
- [41] See, for example, M. Lindner, Z. Phys. 31(1986)295 and references therein.
- [42] T.Hambye and K.Riesselmann, Phys. Rev. D55(1997)7255.
- [43] H. Haber and R. Hempfling, Phys. Rev. Lett. 66(1991)1815; J. Ellis, G. Ridolfi and F. Zwirner, Phys. Lett. B257(1991)83; Y. Okado, M. Yamaguchi and T. Yanagida, Progr. Theor. Phys. Lett. 85(1991)1; R. Barbieri, F. Caravaglios and M. Frigeni, Phys. Lett. B258(1991)167. For a 2-loop improvement, see also: R. Hempfling and A.H. Hoang, Phys. Lett. B331(1994)99.

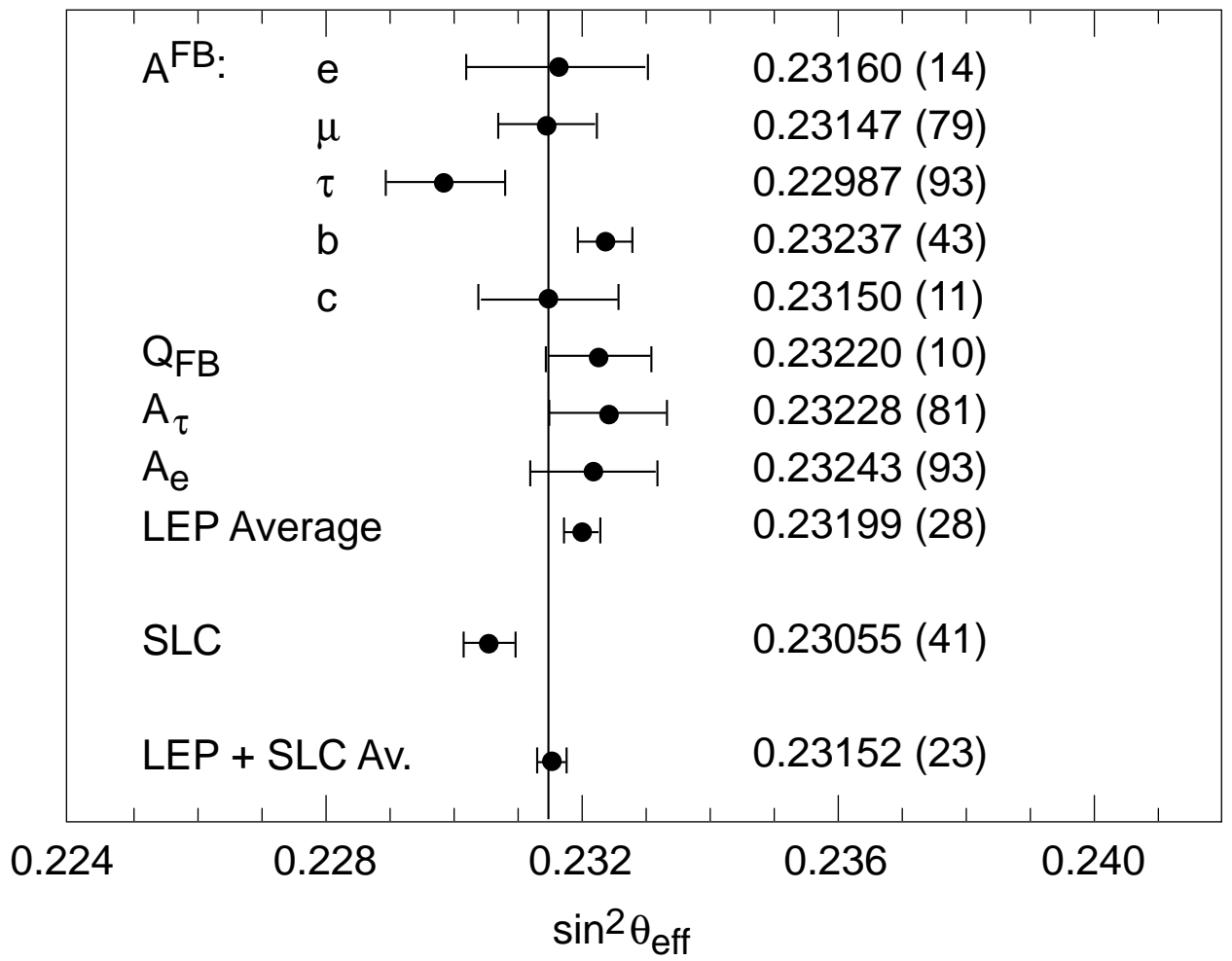


Fig. 1

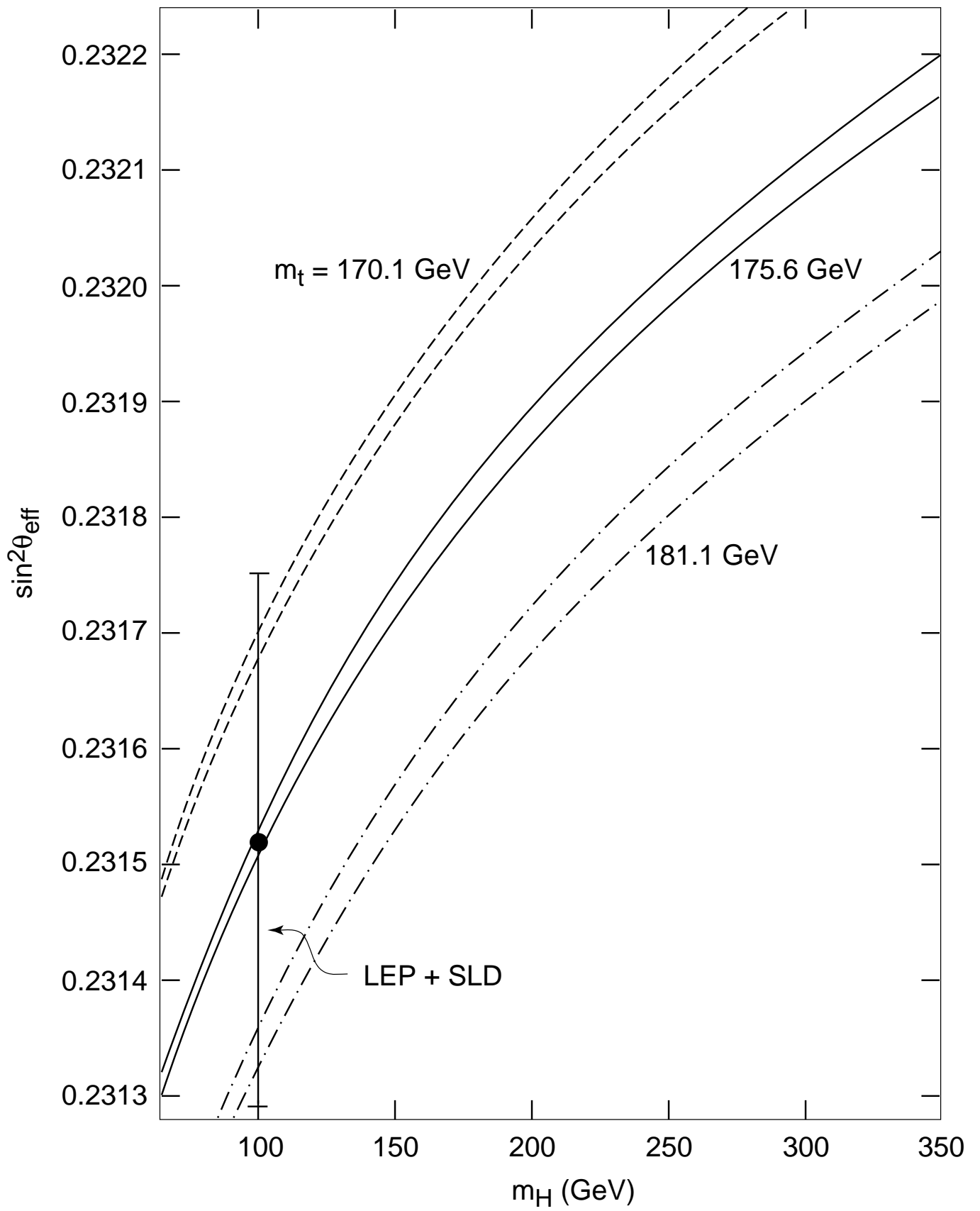


Fig. 2

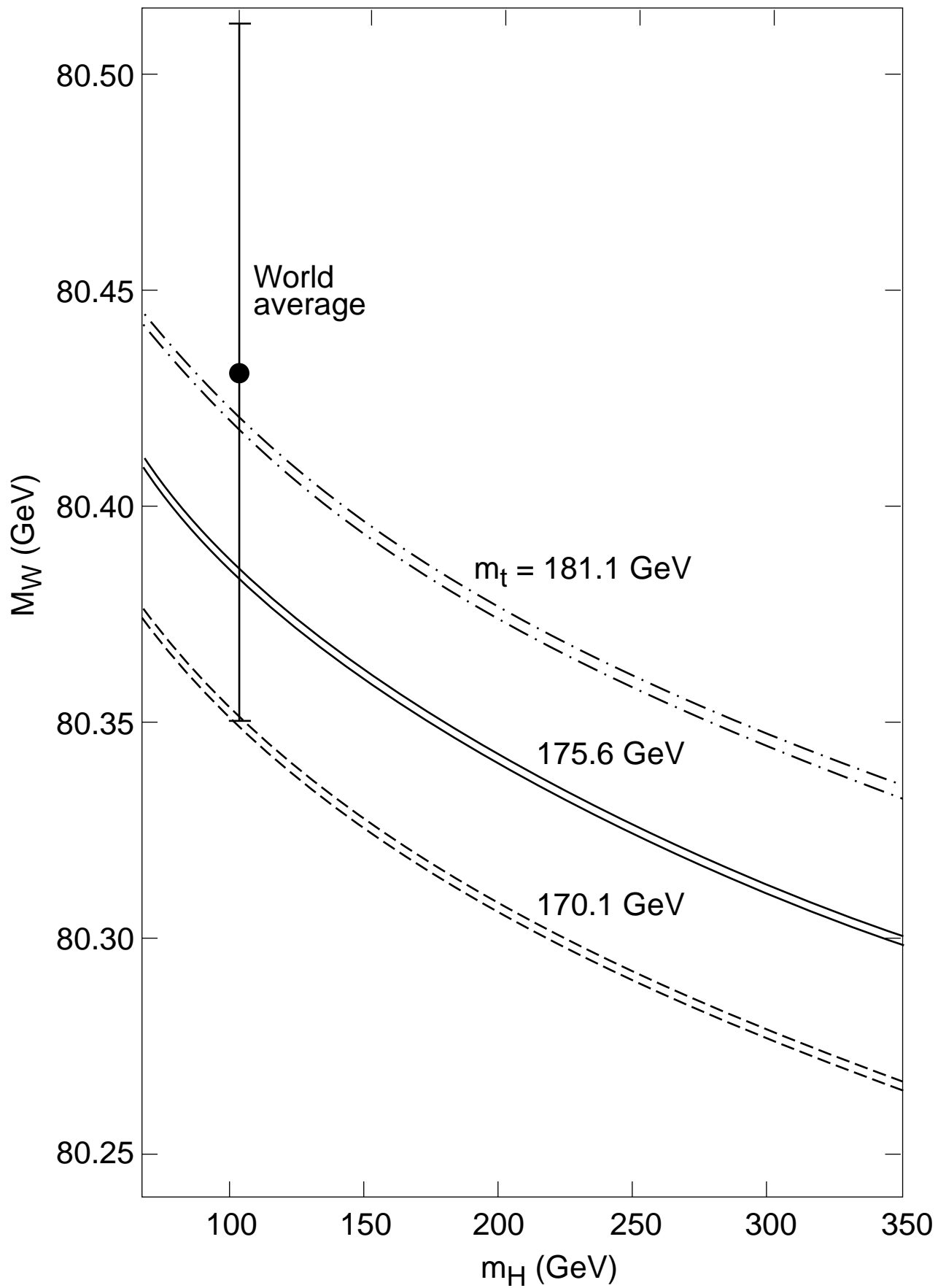


Fig. 3

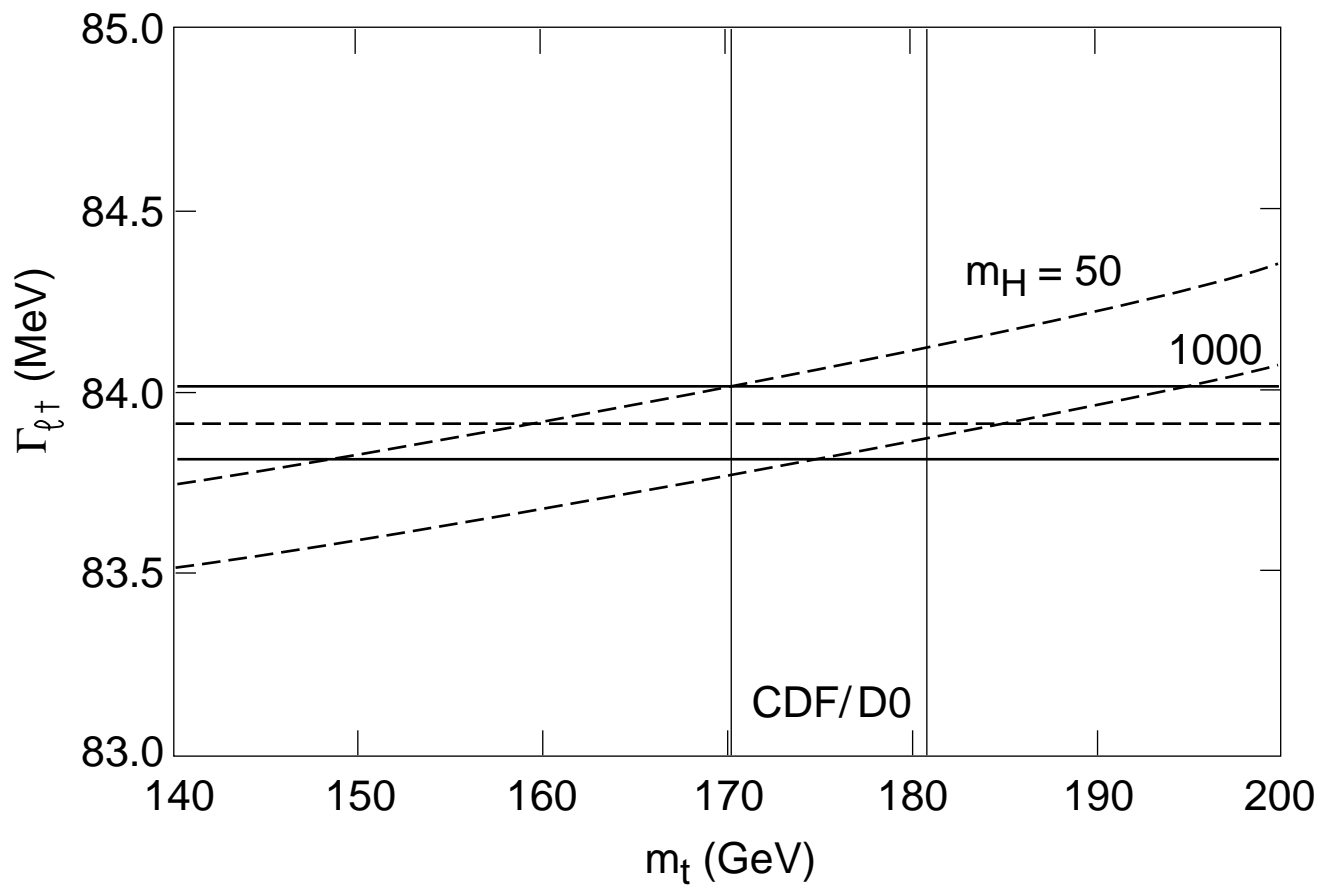


Fig. 4

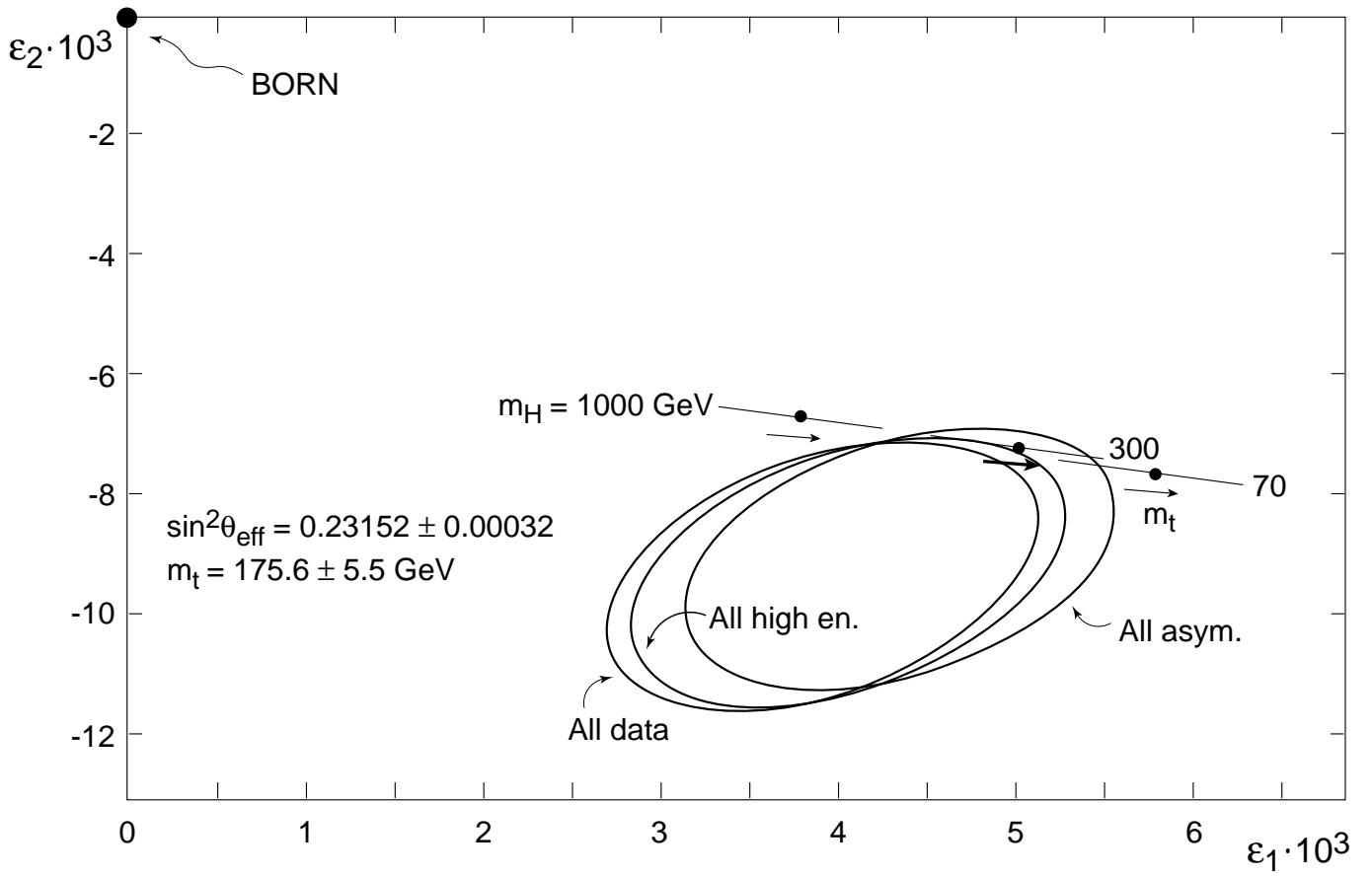


Fig. 5

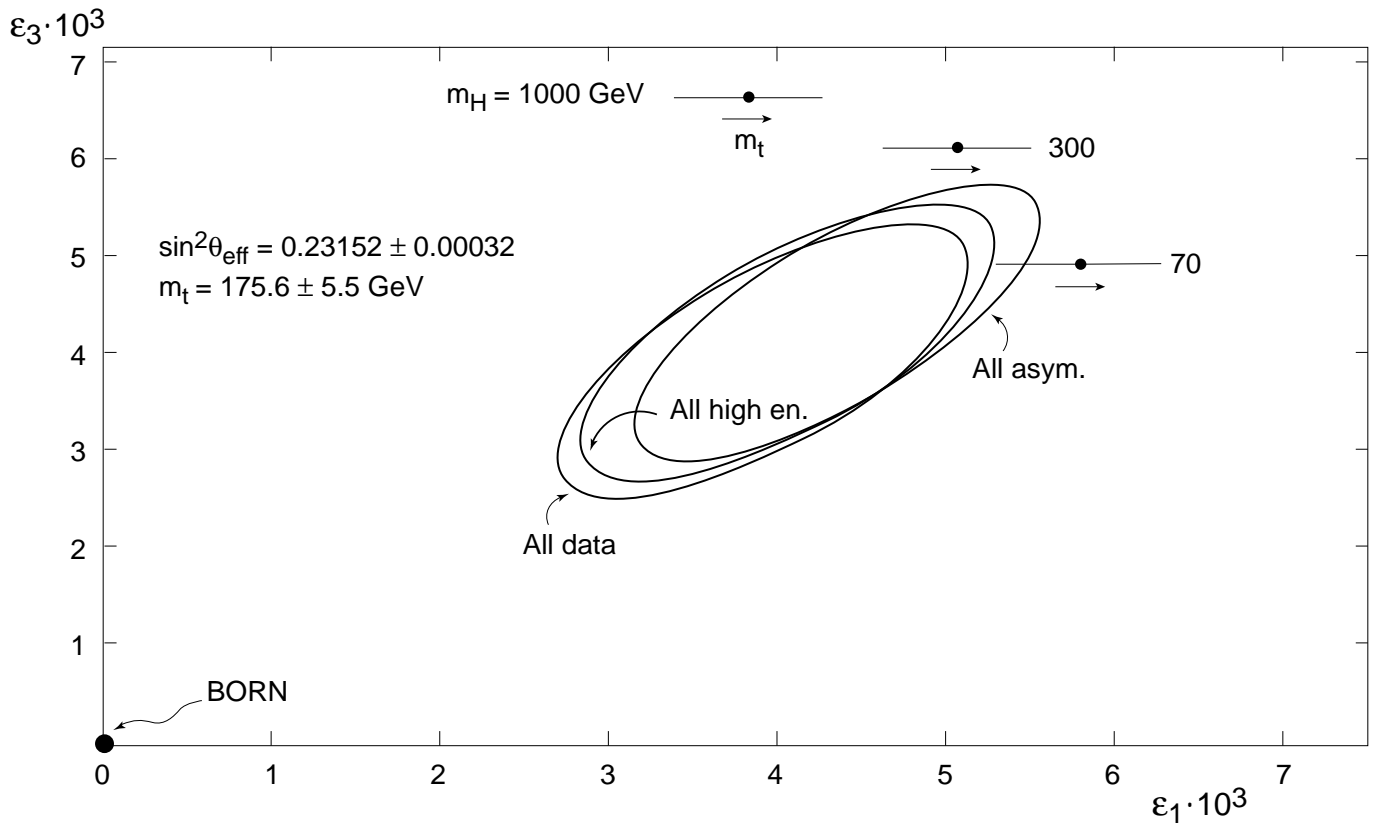


Fig. 6

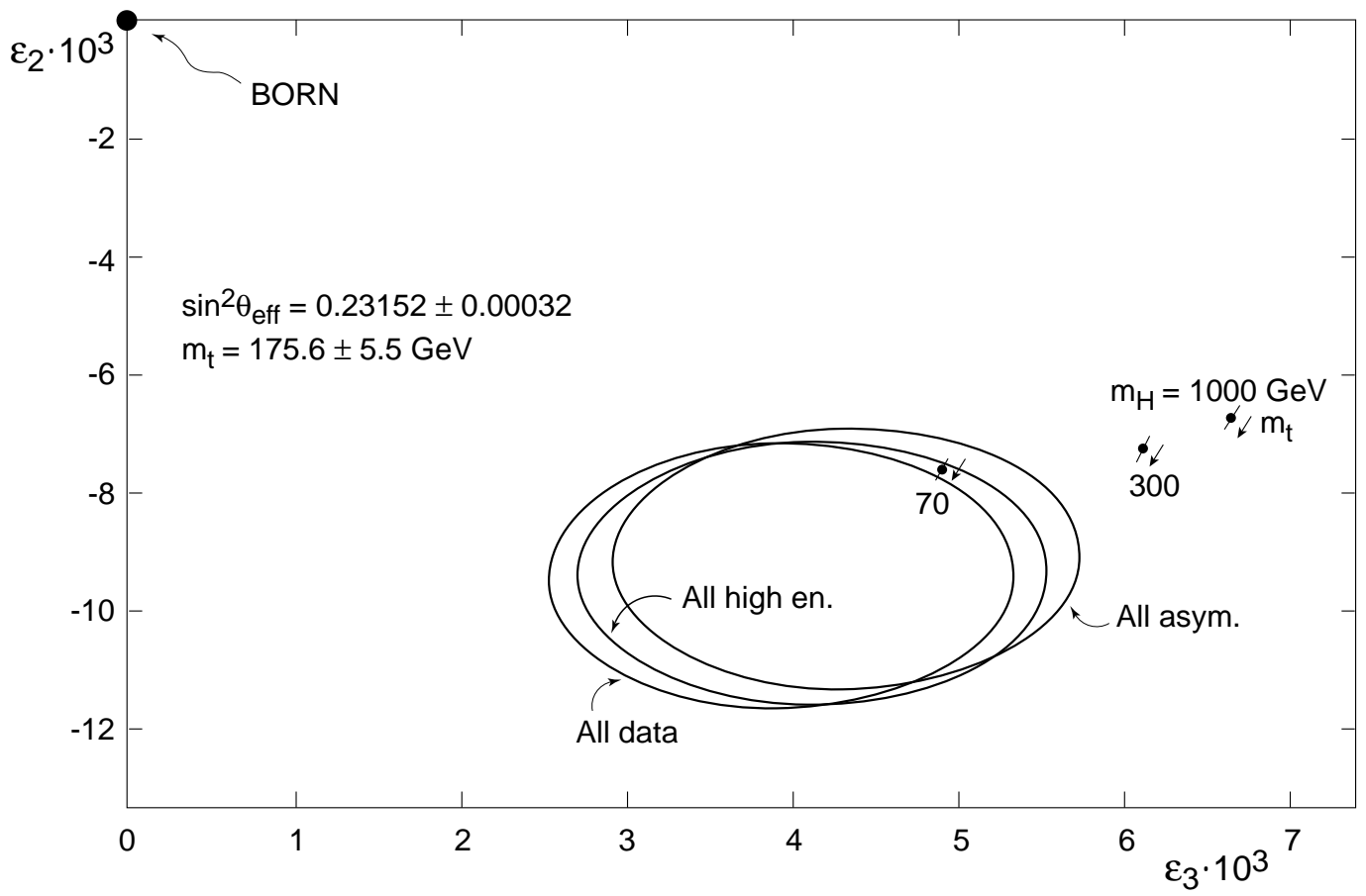


Fig. 7

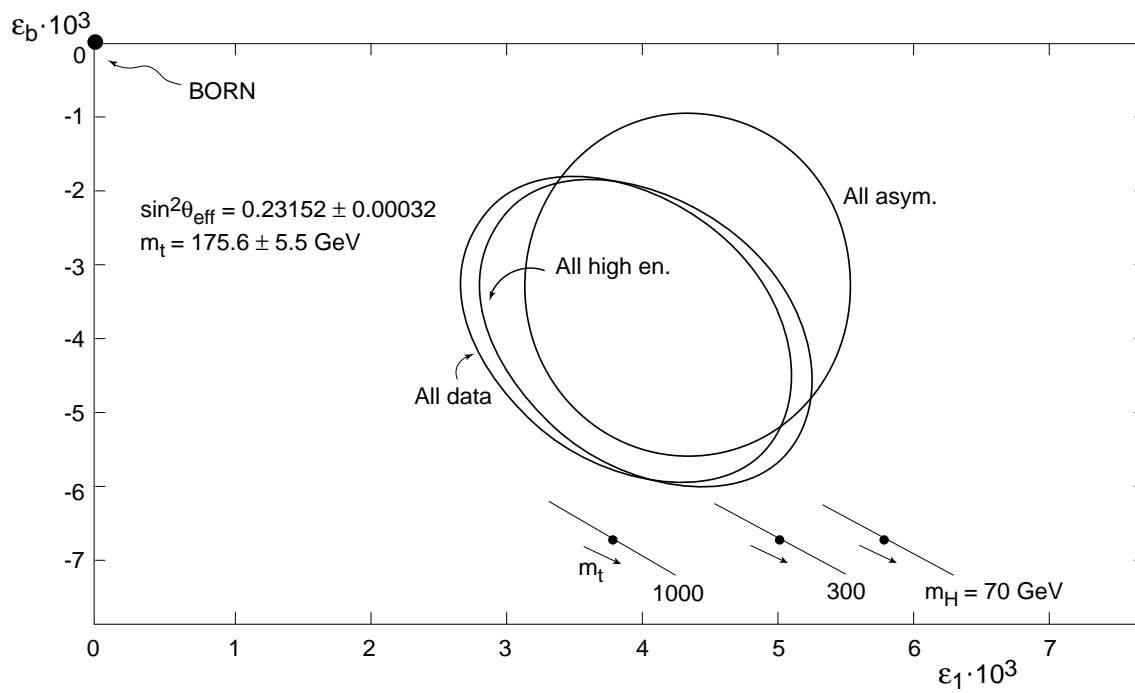


Fig. 8

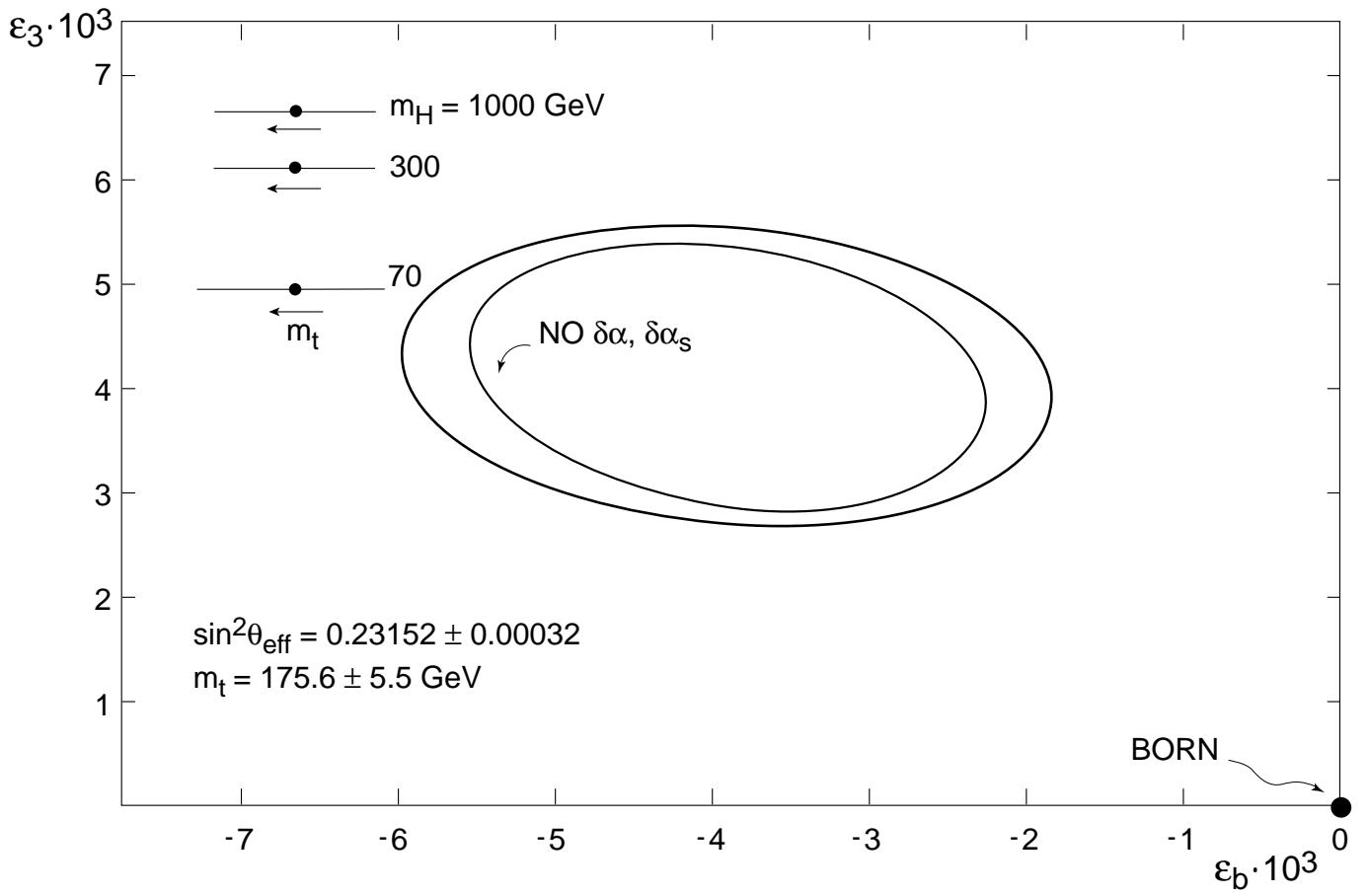


Fig. 9

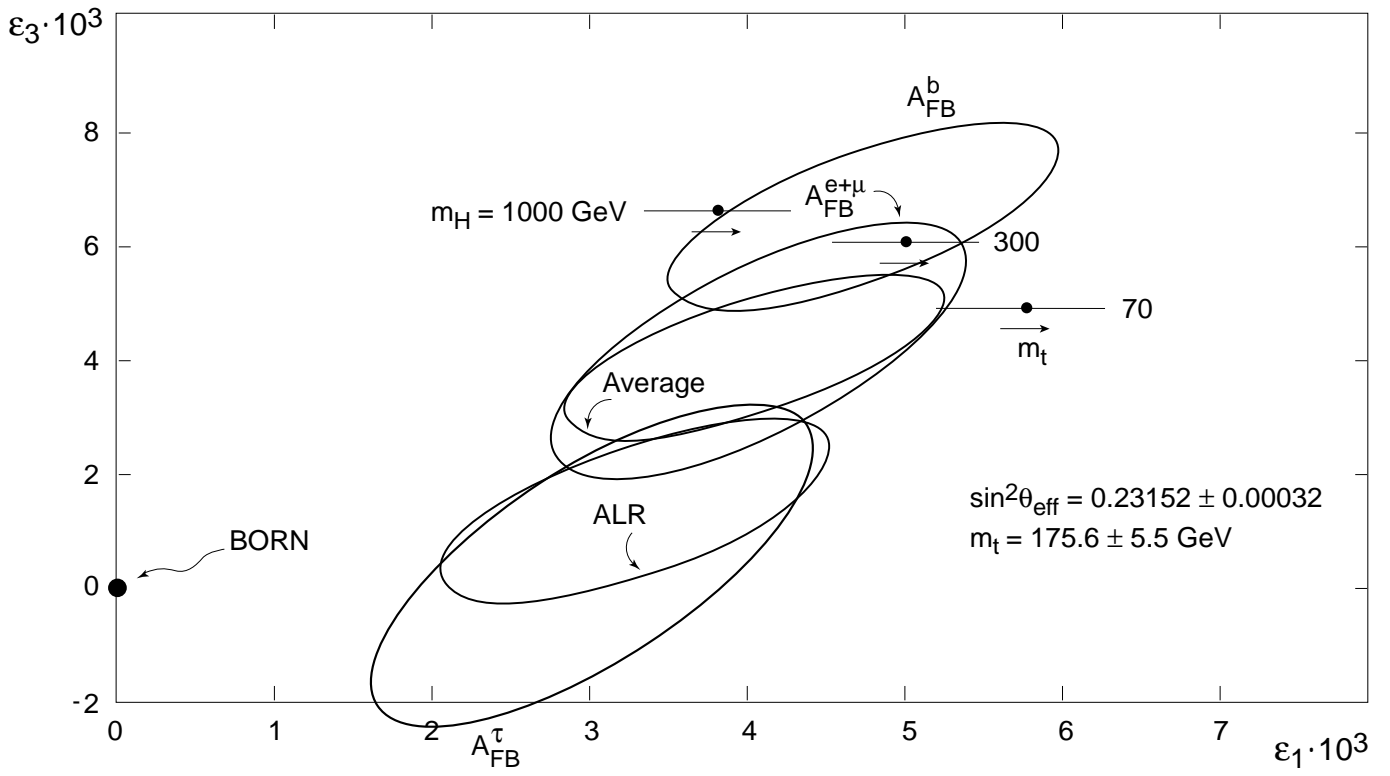


Fig. 10

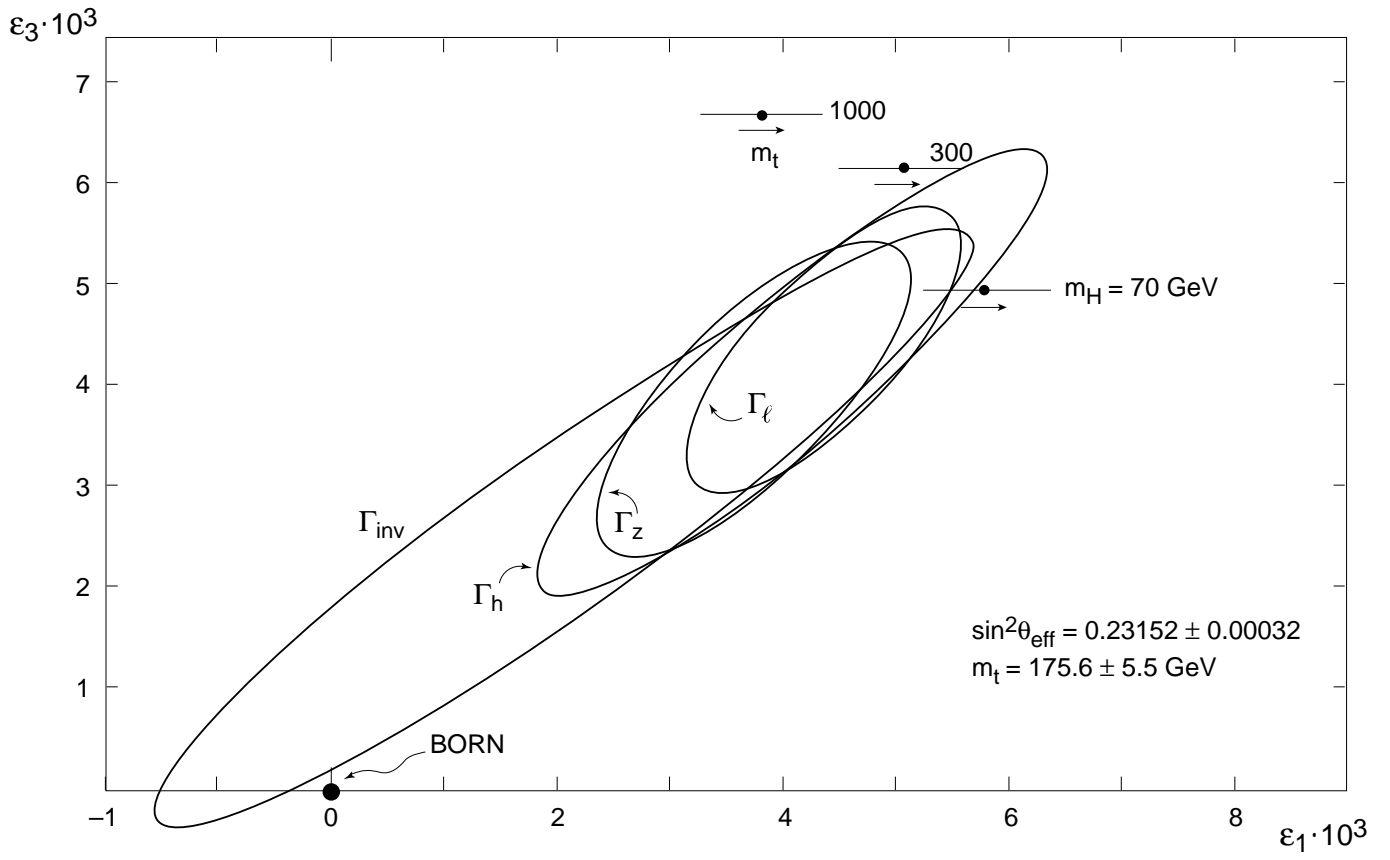


Fig. 11

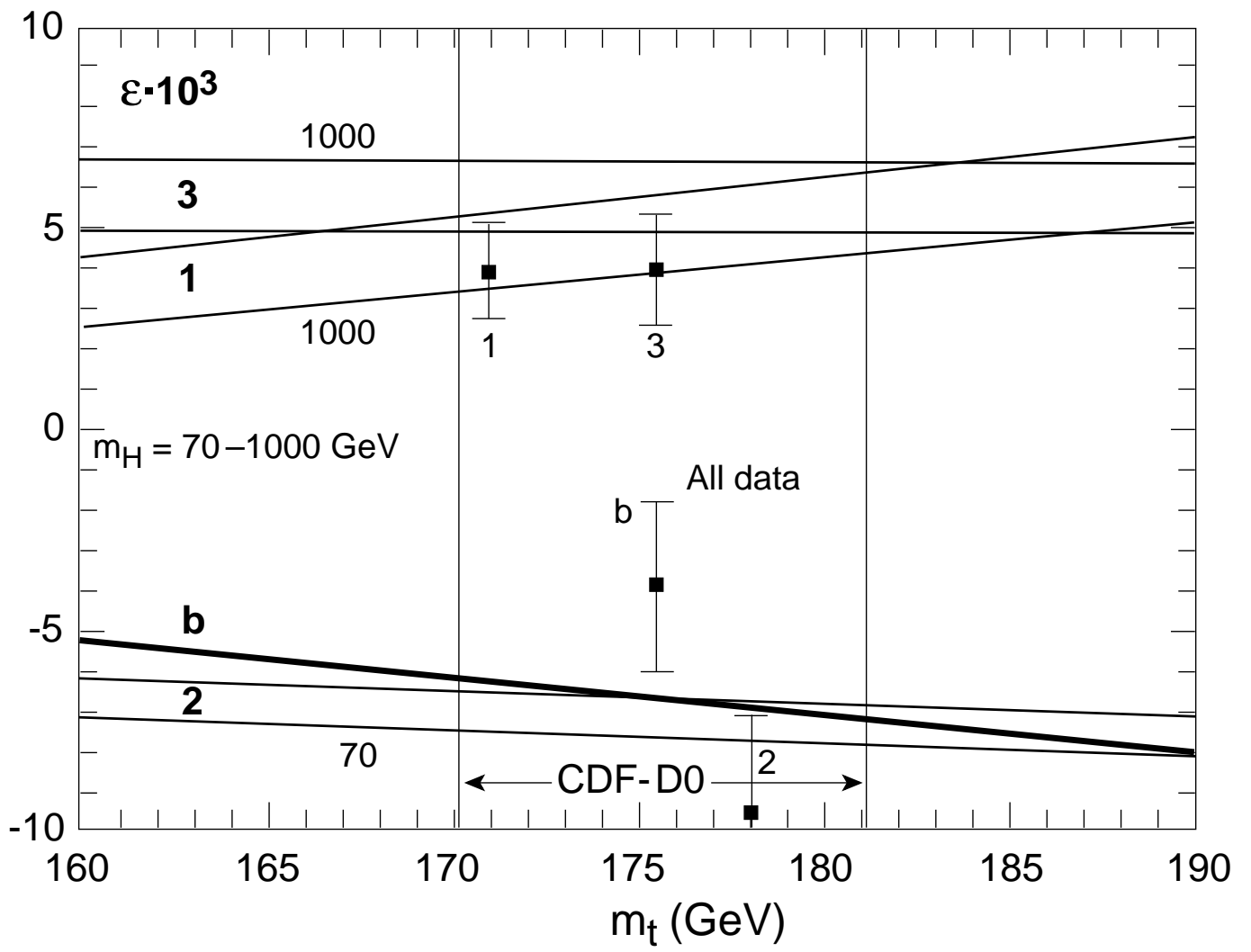


Fig. 12

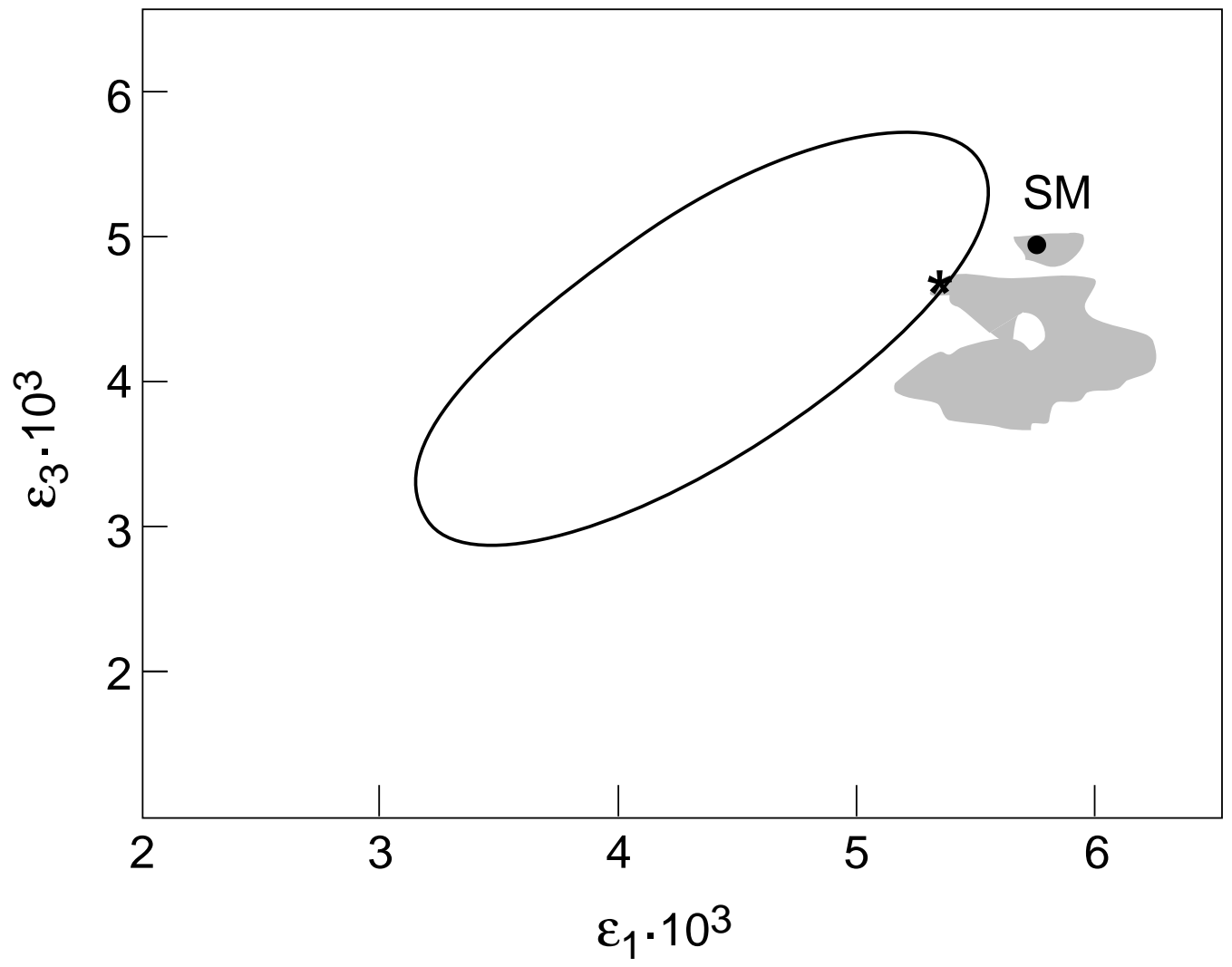


Fig. 13

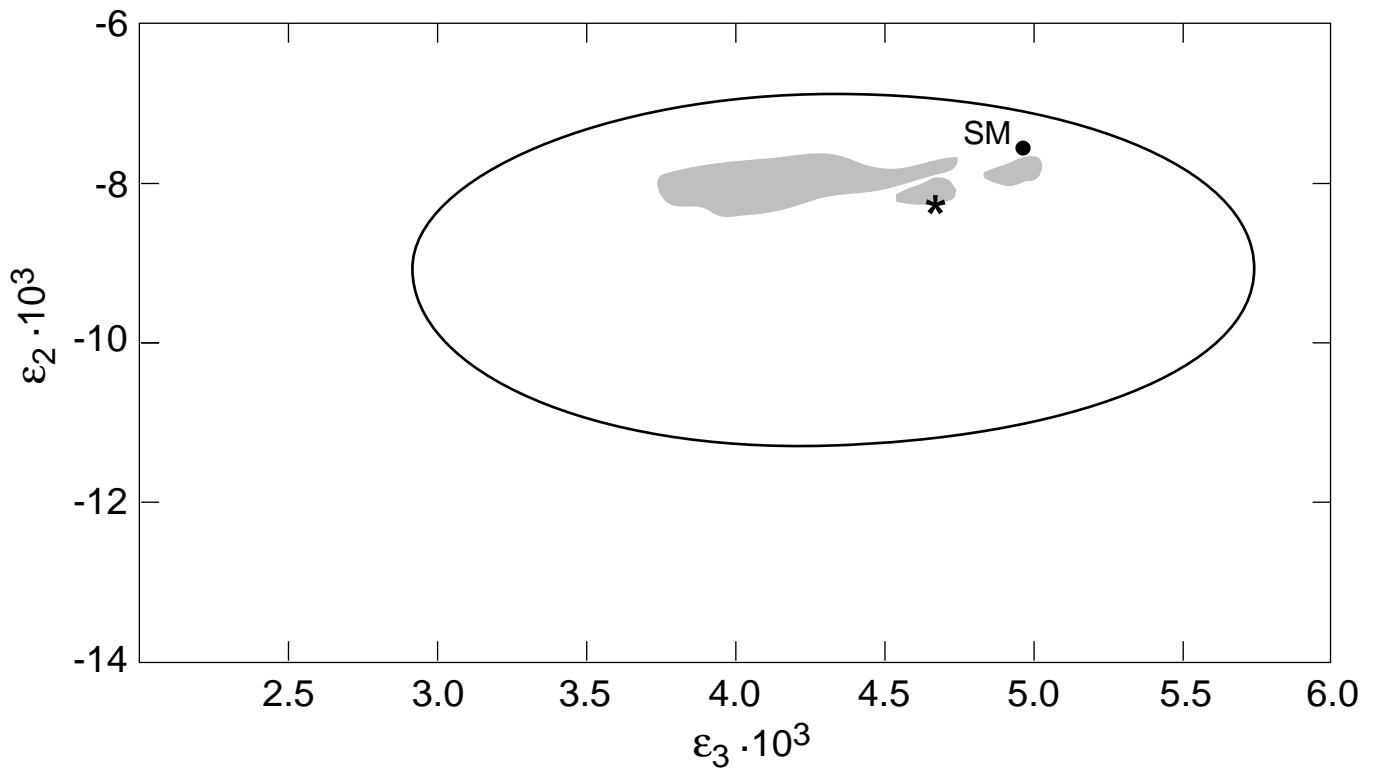


Fig. 14